Diagnostic computation of moisture budgets in the ERA-Interim Reanalysis with reference to analysis of CMIP-archived atmospheric model data

Richard Seager and Naomi Henderson *

Lamont Doherty Earth Observatory of Columbia University, Palisades, New York

* *Corresponding author address:* Richard Seager, Lamont Doherty Earth Observatory of Columbia University, 61 Route 9W., Palisades, NY 10964. Email: seager@ldeo.columbia.edu

Submitted to *Journal of Climate* January 2013, revised April 2013. LDEO Contribution Number xxxx.

ABSTRACT

The diagnostic evaluation of moisture budgets in archived atmosphere model data is examined. Sources of error in diagnostic computation can arise from the use of numerical methods different to those used in the atmosphere model, the time and vertical resolution of the archived data and data availability. These sources of error are assessed using the climatological moisture balance in the European Centre for Medium Range Weather Forecasts Interim Reanalysis (ERA-I) that archives vertically integrated moisture fluxes and convergence. The largest single source of error arises from the diagnostic evaluation of divergence. The chosen second order accurate centered finite difference scheme applied to the actual vertically integrated moisture fluxes leads to significant differences from the ERA-I reported moisture convergence. Using daily, instead of 6 hourly, data leads to an underestimation of the patterns of moisture divergence and convergence by mid-latitude transient eddies. A larger and more widespread error occurs when the vertical resolution of the model data is reduced to the 8 levels that is quite common for daily data archived for the Coupled Model Intercomparison Project (CMIP). Dividing moisture divergence into components due to the divergent flow and advection requires bringing the divergence operator inside the vertical integral which introduces a surface term for which a means of accurate evaluation is developed. The analysis of errors is extended to the case of the spring 1993 Mississippi Valley floods, the causes of which are discussed. For future archiving of data (e.g. by CMIP) it is recommended that monthly means of time step resolution flow-humidity co-variances be archived at high vertical resolution.

1. Introduction

Droughts and floods are some of the main disruptors of human life causing a never ending sequence of death, destruction, suffering, hunger, disease and economic devastation (see references in Cutter et al. (2009)). As climate change driven by rising greenhouse gases proceeds, there will be additional hazards caused by both changes in the natural variability, and changes in the mean precipitation distributions, as some tropical and mid-to-high latitude areas get wetter and subtropical dry areas get drier and expand (Allen and Ingram 2002; Held and Soden 2006; Intergovernmental Panel on Climate Change 2007; Seager et al. 2010b, 2012). As for naturally occurring droughts and floods, changes in the mean precipitation distribution are caused by changes in the transport of water vapor in the atmosphere that create precipitation anomalies that either deprive areas of water or cause an excess. That is, the atmospheric branch of the hydrological cycle is the key phenomena where these risks to human livelihood originate.

Humans, being naturally curious, have long sought to determine the causes of droughts, pluvials and floods relating them to the responsible changes in atmospheric circulation and water vapor transports. However, ultimately, we need to attempt to anticipate such events in advance so that preparations can be made and the worst impacts avoided. This is true both for the case of natural events occurring on the daily to decadal timescale and also for the more slowly evolving effect of hydroclimate change. In both cases, prediction or projection depends on the use of numerical climate models. Understanding then comes into play as a means of assessing how reliable predictions and projections are, given the fidelity with which the models simulate the important processes. For example, drought over southern North America during La Niña events fundamentally depends on moisture divergence anomalies caused by mean flow anomalies (Seager et al. 2005; Seager and Naik 2012) with the latter tightly coupled to changes in the North Pacific storm track (Seager et al. 2010a; Harnik et al. 2010).

Understanding of the causes of floods and droughts and of ongoing hydroclimate change requires a detailed analysis of the atmospheric moisture budget and the linking of this to changes in the atmospheric circulation and, ultimately, the atmospheric and planetary energy budget. This is not very easy to do either in atmospheric models or gridded, model-based, reanalyses of atmospheric observations. In both cases, the models numerically integrate forward a moisture equation designed to best conserve moisture and to preserve a long term mean balance between precipitation, P, surface evaporation, E, and the vertically integrated moisture convergence although, in the case of reanalyses, the moisture field is also constrained, directly or indirectly, by observations. However, analyses of the causes of hydroclimate variability and change are done diagnostically, after the model has run, using saved data from the model. Typically this data includes velocities and specific humidity on a three dimensional spatial grid as well as surface pressure, P and E. The data may be saved at 6-hourly, daily or monthly temporal resolution, but never at the time step of the model, and only rarely are monthly means of co-variances between quantities (themselves evaluated variously using time step, four times daily, daily mean data etc.) saved. Also the data is only sometimes saved on the native model grid and has often been interpolated to standard pressure levels with varying degrees of vertical resolution. Many efforts have been used to diagnose the moisture budget in reanalyses using pressure level data (e.g. Trenberth and Guillemot (1995); Trenberth (1997)). Trenberth and Guillemot (1998) and Seneviratne et al. (2004) recommend performing moisture budget computations at the highest vertical resolution possible on the native model grid. While such data are becoming increasingly available, this is rarely universally practical with archives of data from multiple models such as those within the Coupled Model Intercomparison Project Five (CMIP5, Taylor et al. (2012)).

The task of the researcher is, more commonly, to analyze the causes of hydroclimatic events using these incomplete model data sets. At the simplest level the researcher will then discover that, in the long term mean, the model reported $P - E$ cannot be made to balance the convergence of the vertically integrated moisture flux, no matter how the latter is calculated. However, even if it did balance, this would not be very enlightening. The main goal of such work is to go further and determine what the causes of the moisture convergence or divergence anomalies are and, therefore, break it down into components due to changes in mean circulation, specific humidity and transient eddies (e.g. Huang et al. (2005); Seager et al. (2010b); Seager and Naik (2012); Seager et al. (2012); Nakamura et al. (2012)). To do this requires further analysis of the moisture budget and creates a new set of problems as we shall see.

The point of this paper is to provide a detailed and thorough assessment of the errors introduced in diagnostic analyses of the moisture budget and how these depend on the temporal and spatial resolution of the data and what additional errors are introduced in attempts to break down moisture convergence into constituent parts. We also aim to provide guidance as to the best possible way to numerically evaluate the moisture budget with existing model data and suggest improvements for the archiving of model and reanalysis data in the future that will allow improved accuracy in diagnostic computations. To this effect we will consider the climatological moisture budget and then apply the lessons learned to the moisture budget during a major hydroclimatic anomaly - that of the Mississippi floods of late spring-early summer 1993 - and show that, budget errors notwithstanding, it is possible to use the chosen reanalysis to elucidate the physical mechanisms that led to the flood.

2. Reanalyses data used

For demonstration purposes we use the European Centre for Medium Range Weather Forecasts (ECMWF) Interim Reanalysis (ERA-I) (Berrisford et al. 2011b,a; Dee et al. 2011) which is the latest of the ECMWF Reanalyses. ERA-I covers the post 1979 period. It assimilates cloud and rain-affected satellite irradiances and has a greatly improved representation of the hydrological cycle relative to its precursor, ERA-40. This makes it good for our purpose. Berrisford et al. (2011a) discuss the conservation of moisture in the ERA-I and conclude that mass adjustment of the moisture divergence is not necessary and this was not done to the reported fields. Also ERA-I provides the divergence of the vertically integrated moisture transport as data output, i.e. this provides the actual value of the quantity we are trying to evaluate diagnostically from archived model or reanalysis data. However, it should be noted, in part because of the assimilation scheme, this quantity does not balance the ERA-I $P-E$, even after accounting for the change over time of the vertically integrated specific humidity (see Trenberth et al. (2011)). The ERA-I reanalysis is based on an atmospheric model and reanalysis system with 60 levels in the vertical with a top level at 0.1mb, a T255 spherical harmonic representation and, for surface and grid point fields, a reduced Gaussian grid with an about 79km spacing (Berrisford et al. 2011b). However, the highest resolution calculations reported here are performed on data that was archived by ECMWF on a regular 0.75 degrees grid with 37 model levels. At the time of writing not all the 6 hourly, pressure level data needed for our calculations were available on the 0.75 degree grid. Further it would have been impractical to download and store all the data we needed at this temporal and full spatial resolution and, therefore, for most of the calculations, we use the 1.5 degree longitude by latitude data also archived by ECMWF.

3. Diagnostic computation of the moisture budget in atmosphere models

Most models use a terrain-following vertical co-ordinate. The σ-coordinate, with $p = \sigma p_s$, where p = pressure and p_s its surface values, was the first such coordinate but more commonly used today is a hybrid vertical coordinate, ξ, which preserves $\xi = 0$ at $p = 0$ and $\xi = 1$ at $p = p_s$ but with the pressure at model level k, p_k, given by $p_k = A_k + B_k p_s$ where A_k and B_k are constants. The hybrid vertical coordinate is usually set up to vary from a terrain-following coordinate in the lower troposphere to a p coordinate in the stratosphere. On the other hand model data is commonly archived on standard pressure levels necessitating the use of a p coordinate in diagnostic analysis. To deal with both these vertical coordinate systems we begin with a generalized vertical coordinate, η (see Konor and Arakawa (1997)), for which the material derivative of a quantity is given by:

$$\frac{D}{Dt} = \left(\frac{\partial}{\partial t}\right)_\eta + \mathbf{u} \cdot \nabla_\eta + \dot{\eta}\frac{\partial}{\partial \eta} \tag{1}$$

where $\dot{\eta} = D\eta/Dt$.

In this vertical coordinate the moisture equation is (dropping η subscripts):

$$\frac{\partial q}{\partial t} + \nabla \cdot (\mathbf{u}q) + \dot{\eta}\frac{\partial q}{\partial \eta} = e - c \tag{2}$$

where q is specific humidity and $\mathbf{u}$ is the velocity vector along η surfaces and e and c are evaporation and condensation. We use spherical coordinates so the divergence of moisture is given by:

$$\nabla \cdot (\mathbf{u}q) = \frac{1}{a\cos\phi}\left(\frac{\partial(uq)}{\partial\lambda} + \frac{\partial(vq\cos\phi)}{\partial\phi}\right), \tag{3}$$

where u and v are the zonal and meridional components of velocity, a is the radius of the Earth, λ is longitude and ϕ is latitude. The continuity equation is:

$$\frac{\partial}{\partial t}\frac{\partial p}{\partial \eta} + \nabla \cdot \left(\mathbf{u}\frac{\partial p}{\partial \eta}\right) + \frac{\partial}{\partial \eta}\left(\dot{\eta}\frac{\partial p}{\partial \eta}\right) = 0. \tag{4}$$

These can be combined into the flux form of the humidity equation:

$$\frac{\partial}{\partial t}\left(q\frac{\partial p}{\partial \eta}\right) + \nabla \cdot \left(\mathbf{u}q\frac{\partial p}{\partial \eta}\right) + \frac{\partial}{\partial \eta}\left(q\dot{\eta}\frac{\partial p}{\partial \eta}\right) = \frac{\partial p}{\partial \eta}(e-c) \tag{5}$$

This equation can be vertically integrated to derive a relation for the precipitation minus surface evaporation $P-E$:

$$P - E = -\frac{1}{g\rho_w}\int_0^1 \frac{\partial}{\partial t}\left(q\frac{\partial p}{\partial \eta}\right) d\eta - \frac{1}{g\rho_w}\int_0^1 \nabla \cdot \left(\mathbf{u}q\frac{\partial p}{\partial \eta}\right) d\eta, \tag{6}$$

where g is the acceleration due to gravity and ρ_w is the density of water, the inclusion of which mean that $P-E$ is in units of ms^{-1} (or mm/day as will be shown in the figures). Since the limits of integration on η are independent of space and time this can be rewritten with the time derivative and divergence operator outside of the integral as:

$$P - E = -\frac{1}{g\rho_w}\frac{\partial}{\partial t}\int_0^1 \left(q\frac{\partial p}{\partial \eta}\right) d\eta - \frac{1}{g\rho_w}\nabla \cdot \int_0^1 \left(\mathbf{u}q\frac{\partial p}{\partial \eta}\right) d\eta. \tag{7}$$

In the case of data provided on pressure levels we revert to a p coordinate for which Eq. 5 becomes:

$$\frac{\partial q}{\partial t} + \nabla \cdot (\mathbf{u}q) + \frac{\partial}{\partial p}(\omega q) = e - c \tag{8}$$

The p-coordinate flux form moisture equation can be vertically integrated from the surface pressure, p_s, to the top of the atmosphere to derive:

$$P - E = -\frac{1}{g\rho_w}\int_0^{p_s} \frac{\partial q}{\partial t} dp - \frac{1}{g\rho_w}\int_0^{p_s} \nabla \cdot (\mathbf{u}q)\, dp - \frac{1}{g\rho_w}\omega_s q_s, \tag{9}$$

where the subscript s refers to surface quantities. Noting that:

$$\omega_s = \frac{\partial p_s}{\partial t} + \mathbf{u}_s \cdot \nabla p_s, \tag{10}$$

$$\int_0^{p_s} \frac{\partial q}{\partial t} dp = \frac{\partial}{\partial t} \int_0^{p_s} q dp - q_s \frac{\partial p_s}{\partial t}, \tag{11}$$

$$\int_0^{p_s} \nabla \cdot (\mathbf{u} q)\, dp = \nabla \cdot \int_0^{p_s} \mathbf{u} q dp - q_s \mathbf{u}_s \cdot \nabla p_s, \tag{12}$$

we derive:

$$P - E = -\frac{1}{g\rho_w} \frac{\partial}{\partial t} \int_0^{p_s} q dp - \frac{1}{g\rho_w} \nabla \cdot \int_0^{p_s} \mathbf{u} q dp. \tag{13}$$

This is the form of the moisture budget equation that we focus most of the analysis on. However, this form only allows understanding of the moisture budget (and its variations) to advance so far. Note that the divergence operates on the vertically integrated moisture field and does not allow a breakdown of the moisture convergence into a part due to the mass convergence and a part due to advection of humidity gradients. Therefore an alternative form is often presented:

$$P - E = -\frac{1}{g\rho_w} \frac{\partial}{\partial t} \int_0^{p_s} q dp - \frac{1}{g\rho_w} \int_0^{p_s} \nabla \cdot (\mathbf{u} q) dp - \frac{1}{g\rho_w} q_s \mathbf{u}_s \cdot \nabla p_s, \tag{14}$$

which allows the divergence to be broken down into parts related to a divergent flow $q\nabla \cdot \mathbf{u}$ and a part related to advection $\mathbf{u} \cdot \nabla q$, viz.

$$P - E = -\frac{1}{g\rho_w} \frac{\partial}{\partial t} \int_0^{p_s} q dp - \frac{1}{g\rho_w} \int_0^{p_s} (q\nabla \cdot \mathbf{u} + \mathbf{u} \cdot \nabla q)\, dp - \frac{1}{g\rho_w} q_s \mathbf{u}_s \cdot \nabla p_s. \tag{15}$$

Here the separation into components of moisture divergence due to divergent flow and advection is only allowed by bringing the divergence operater inside the vertical integral and, hence, introduces a boundary term, $q_s \mathbf{u}_s \cdot \nabla p_s$, that also needs to be accounted for (and which is sometimes discussed (Seager and Vecchi 2010; Seager et al. 2010b) but which is also often ignored (Seager et al. 2007)).

These equations have been written in continuous form but in models will be evaluated using various numerical methods. For example the model that ERA-I is based upon uses a finite difference method to evaluate vertical derivatives and a semi-Lagrangian method to determine advective tendencies (ECMWF 2012). Other models use three dimensional semi-Lagrangian methods. The humidity tendencies induced by these schemes cannot be reproduced using archived data that already include the effect of the advection even if the data were archived at the model time step. A numerical method needs to be chosen to evaluate the terms in the moisture equation with the additional goal that it is general enough to be applicable to a variety of reanalyses and/or models.

The vertically integrated moisture transport is approximated by:

$$\int_0^{p_s} (\mathbf{u}q)\, dp \approx \sum_{k=1}^{K_{i,j}} \mathbf{u}_k q_k \Delta p_k \tag{16}$$

where the summation is over vertical layers, k, of which there are $K_{i,j}$ with i and j indicating the longitude and latitude location of grid points. In the original η coordinates $K_{i,j}$ is the same at all grid points but for archived pressure level data $K_{i,j}$ will depend on longitude and latitude. The divergence operator on a two-dimensional vector $\mathbf{F}$ is evaluated via:

$$\begin{aligned}\nabla_f \cdot \mathbf{F} \approx \frac{1}{a\cos\phi_j}\Bigg\{ \frac{1}{\lambda_{i+1,j}-\lambda_{i-1,j}} \Bigg[(\lambda_{i,j}-\lambda_{i-1,j}) \frac{F^{\lambda}_{i+1,j}-F^{\lambda}_{i,j}}{\lambda_{i+1,j}-\lambda_{i,j}} + \\ (\lambda_{i+1,j}-\lambda_{i,j}) \frac{F^{\lambda}_{i,j}-F^{\lambda}_{i-1,j}}{\lambda_{i,j}-\lambda_{i-1,j}} \Bigg] + \frac{1}{\phi_{i,j+1}-\phi_{i,j-1}} \Bigg[(\phi_{i,j}-\phi_{i,j-1}) \frac{\cos\phi_{j+1}F^{\phi}_{i,j+1}-\cos\phi_j F^{\phi}_{i,j}}{\phi_{i,j+1}-\phi_{i,j}} + \\ (\phi_{i,j+1}-\phi_{i,j}) \frac{\cos\phi_j F^{\phi}_{i,j}-\cos\phi_{j-1}F^{\phi}_{i,j-1}}{\phi_{i,j}-\phi_{i,j-1}} \Bigg] \Bigg\}\end{aligned} \tag{17}$$

where F^{λ} and F^{ϕ} indicate the components of $\mathbf{F}$ in the longitude and latitude directions and ∇_f is used to indicate a finite difference approximation to the divergence operator on a longitude-latitude grid. To evaluate moisture divergence, $\mathbf{F}_{i,j}$ is given by:

$$\mathbf{F}_{i,j} = \sum_{k=1}^{K_{i,j}} \mathbf{u}_{i,j,k} q_{i,j,k} \Delta p_{i,j,k}, \tag{18}$$

To evaluate the divergence at grid point (i,j), Eq. 17 computes centered differences at mid-points to the east and west and north and south and then linearly interpolates these in the λ and ϕ directions back to the (i,j) point. This therefore allows for the case of uneven grid spacing (quite common in CMIP models in the ϕ direction). In the case of an even grid, which the ERA-I data is served on, Eq. 17 reduces to the familiar form:

$$\nabla_f \cdot \mathbf{F} \approx \frac{1}{a\cos\phi_j}\left(\frac{F^{\lambda}_{i+1,j} - F^{\lambda}_{i-1,j}}{\lambda_{i+1,j} - \lambda_{i-1,j}} + \frac{\cos\phi_{j+1}F^{\phi}_{i,j+1} - \cos\phi_{j-1}F^{\phi}_{i,j-1}}{\phi_{i,j+1} - \phi_{i,j-1}}\right) \tag{19}$$

The vertical integration goes down to the surface pressure as follows. The pressure thickness of the lowest layer is equal to the surface pressure minus the pressure at the first reported pressure level above and, within this layer, the values of $\mathbf{u}$ and q used are the ones of the first pressure level above the surface pressure value. All of these integration and differentiation approximations introduce errors. In addition, the time resolution of the diagnostic computation will also causes errors if it does not conform to the actual time step of the model. For example a calculation done with 6 hourly data would be expected to be more accurate than one done with daily data.

4. Evaluation of sources of error in diagnostic moisture budget calculations

Here we assess the relative importance of the approximations introduced into diagnostic computation of moisture budgets as detailed in the prior section.

a. Patterns of $P - E$ and divergence of ERA-I reported vertically integrated moisture divergence

First of all the ERA-I reports within its' data archive what is called the vertically integrated moisture divergence which we label MC after multiplying by -1 to convert to moisture convergence. ERA-I also reports the vertically integrated moisture flux which we label $VIMF$. These correspond to:

$$\begin{aligned} MC &= -\frac{1}{g\rho_w}\sum_{k=1}^{K}\nabla\cdot\left(\mathbf{u}q\frac{\partial p}{\partial\eta}\Delta\eta\right)_k \\ &= -\frac{1}{g\rho_w}\nabla\cdot\sum_{k=1}^{K}\left(\mathbf{u}q\frac{\partial p}{\partial\eta}\Delta\eta\right)_k \\ &= -\frac{1}{g\rho_w}\nabla\cdot VIMF \end{aligned} \tag{20}$$

with the vertical sum done on the model η grid, as indicated by use of $\frac{\partial p}{\partial \eta}\Delta\eta$, over the K model layers. Note that since this is evaluated on the model η grid it does not matter whether the divergence operator is inside or outside the vertical sum. ECMWF report MC and $VIMF$ as both monthly means of daily means and also as 6 hourly values with the daily mean equal to the average of the four 6 hourly values within that day. Using a double overbar to indicate climatological monthly means, Figure 1 shows the climatological monthly means for January and July of $\overline{\overline{MC}}$ and precipitation minus evaporation, $\overline{\overline{P-E}}$, for the ERA-I reanalysis data set, as well as their difference. Not surprisingly there is a rather close balance between these two but the difference shows that this is not a perfect match by any means. In reality vertically integrated moisture divergence on the model grid should differ from $P-E$ by the change in vertically integrated moisture (Eq. 7). Hence we also show this in Figure 1 where it is evaluated for each month as the ERA-I reported vertically integrated moisture content for the first day of the next month minus that for the first of the month itself. The change in moisture storage shows the expected seasonal cycle (moistening in the summer hemisphere, drying in the winter hemisphere) but this pattern is quite different from the $\overline{\overline{P-E}} - \overline{\overline{MC}}$ one. The imbalance is very similar in pattern to that shown by Berrisford et al. (2011a).

Consequently, even though the Reanalysis reports a vertically integrated moisture divergence, this does not balance the sum of model $\overline{\overline{P-E}}$ and change in moisture storage. There are three possible reasons for this. One is that Eq. 20 is an approximation to the moisture convergence the model effectively sees. This is because the ECMWF model actually updates its humidity field by applying a semi-Lagrangian scheme to an advective form of the moisture equation. As such moisture divergence does not need to be evaluated in the updating of the model. In contrast, to derive MC as a diagnostic, the moisture divergence is evaluated in spectral space the same way that mass divergence is computed in the model to evaluate vertical velocities (Berrisford et al. 2011a). Another reason for an imbalance is that the ECMWF model contains a moisture diffusion along η surfaces (ECMWF 2012) but the q tendencies induced by this are not saved or known (and also cannot be computed from the humidity field after the fact). The third reason is that the reported P, E, q and MC fields have been influenced by the data assimilation scheme such that the moisture budget (Eq. 6) need no longer be in balance because of so-called 'analysis increments' (Trenberth et al. 2011).

b. Error introduced in evaluation of time mean divergence of vertically integrated moisture flux

The imbalance between $P - E$, moisture storage and MC in ERA-I is not of immediate concern to us. In climate models these will balance more closely because the moisture budget is closed due to the absence of analysis increments. Hence our main effort is to assess how well the divergence of vertically integrated moisture can be evaluated diagnostically using archived data. That is, how well can the ERA-I reported MC itself be approximated from archived $\mathbf{u}$ and q on pressure levels together with p_s? As discussed, errors will be introduced in the evaluation of the divergence, in the evaluation of the vertical integral and by the time resolution of the data, each of which will be treated in turn.

1) Error from evaluation of divergence

ERA-I reports the vertical integral of moisture flux, $VIMF$, and its convergence, MC. Hence by applying to $VIMF$ the simple centered difference divergence operator as in Eq. 17 we determine the error introduced relative to the ERA-I reported value. That is we evaluate:

$$-\frac{1}{g\rho_w}\nabla \cdot \overline{\overline{VIMF}} \quad c.f. \quad -\frac{1}{g\rho_w}\nabla_f \cdot \overline{\overline{VIMF}}$$

Figure 2 shows this difference. Most of the analyses to follow are on the 1.5 degree grid and these results are shown in the middle row of Figure 2. The difference between the 1.5 degree actual and diagnosed convergence is considerably larger than any subsequent errors introduced through decreases in temporal or vertical resolution. Errors introduced by the divergence operator approximation are concentrated in regions where the spatial gradients in the moisture convergence field are large. This is expected as the errors in the ∇_f approximation will appear like derivatives of the divergence field. For example the Pacific and Atlantic Intertropical Convergence Zones (ITCZs), where the moisture convergence varies in strength and sign over small meridional distances, are regions of notable error. Coastal regions, where the moisture convergence also has strong gradients, and mountainous regions are other areas where the divergence approximation introduces notable errors.

The top row of Figure 2 shows the same difference between reported and diagnosed moisture convergence when the 0.75 degree grid data is used. This is much smaller than the error using the coarse resolution data and makes clear that discretization error is a major source of error in the latter. However, even at the higher resolution, sizable errors in the diagnostic calculation occur, especially over land and regions of severe topography. To assess how coherent the errors are, in the bottom row of Figure 2 we show a version of the error with the 1.5 degree grid after one pass of a 1-2-1 spatial smoother. This effectively removes a lot of the error, as expected if it arises from discretization error, but notably leaves errors near key climatic features like the ITCZ.

Table 1 shows the climatological area averages of root mean square differences between monthly means of $-\frac{1}{g\rho_w}\nabla_f \cdot \overline{\overline{VIMF}}$ and both $\overline{\overline{MC}}$ and the convergence of vertically integrated moisture as computed by us. These are all for the 1.5 degrees grid. It can be seen there that the largest error comes from the comparison of $\overline{\overline{MC}}$ with $-\frac{1}{g\rho_w}\nabla_f \cdot \overline{\overline{VIMF}}$, i.e. purely from the evaluation of divergence. The other root mean square errors in Table 1 are between quantities in which for both the divergence is computed by us as in Eq. 17 (see below) and therefore include only errors due to time or vertical resolution of that data. These are smaller than the error introduced by the divergence evaluation. This error can be made smaller by applying the finite difference divergence operator to data closer to the actual model resolution but not entirely removed. It should be recalled that moisture convergence is never actually computed during integration of the model so it is not clear what the actual truth is and some level of disagreement has to accepted. The issue then becomes the extent to which it impacts any analysis of interest, a matter we address later.

2) Error introduced from using time resolution of archived data

We begin by considering how the moisture balance is impacted by the fact that the archived data are not at the model time step but are instead stored at the 6 hourly or, perhaps, daily timescale. In the case of ERA-I the data are 6 hourly and hence ignore the co-variance of $\mathbf{u}$ and q at shorter timescales. To do this we show in Figure 3 the quantity:

$$-\frac{1}{g\rho_w}\nabla_f \cdot \sum_{k=1}^{K} \overline{\overline{\mathbf{u}_{6,k} q_{6,k} \Delta p_{6,k}}} - \overline{\overline{MC}}$$

where the i, j subscripts have been dropped for simplicity and the '6' subscript indicates that this is evaluated using 6-hourly data for $\mathbf{u}, q$ and p. In this case errors are introduced both by the reduced time resolution of the data and by the vertical integration being performed by us (on 26 levels) rather than by ECMWF in a way presumably consistent with the model numerics. Quantitatively, the root mean square differences between the various diagnostic estimates of climatological MC and the actual ERA-I reported values are given in Table 2. There it can be seen, by comparison to Table 1, that $\overline{\overline{MC}}$ is actually closer to the divergence of our vertically integrated moisture flux than it is to the divergence of the ERA-I reported vertically integrated moisture flux. This is something we cannot explain though it implies compensating errors in our computation of divergence and vertical integrals. Despite this nagging issue, Figure 3 shows that, apart from a hint of systematic error near the ITCZ, the errors from time resolution and vertical integration appear randomly scattered around the globe. The ITCZ errors may be due to the existence in that region of transient storm systems with co-varying winds and humidity on the less than 6 hourly timescale.

Figure 3 also shows the quantity:

$$-\frac{1}{g\rho_w}\nabla_f \cdot \sum_{k=1}^{K} \overline{\overline{\mathbf{u}_{d,k} q_{d,k} \Delta p_{d,k}}} - \overline{\overline{MC}}$$

where the d subscript indicates this was evaluated with daily data. In this case errors are systematic with too little moisture divergence at the subtropical edge of the mid-latitudes and too little moisture convergence in the mid-to-high latitudes. This clearly represents an underestimation of poleward moisture transport by mid-latitude transient eddies with the error arising from not sampling the sub–daily co-variance between the flow and the humidity. Since these mid-latitude storms have characteristic timescales of a few to several days it is reasonable that daily resolution data will be inadequate to capture their effects. This point is made clear in Figure 3 where we show the difference between the 6-hourly and daily moisture convergence with the former having stronger subtropical to mid-latitude moisture transport with divergence on the subtropical side and convergence on the poleward side.

3) Error from vertical integration using fewer pressure levels

The calculations so far in which we performed the vertical integration used 26 vertical levels which is more than is often available in archives of model data. Hence we redo the integrations with daily data but with a degraded 18 level data set which has fewer model levels near the surface. Figure 4 shows the difference between a 18 layer vertical integration of the moisture convergence and $\overline{\overline{MC}}$, (which can be compared with Figure 3 for the 26 layer case) and the difference between the 26 and 18 layer integrations, all using daily data. As expected, the errors are in general larger when using fewer layers but these are restricted to land while differences over the ocean are small (also see Table 3). The increased error over land is because of less resolution in the lower atmosphere where the moisture is located and also where vertical gradients of moisture are often large.

6-hourly data is really required for evaluating the transient contributions to moisture budgets but archiving 6-hourly, or even daily, data for complete model runs at model vertical resolution places a considerable stress on data storage requirements and, once archived, on networks used to transfer data from the modeling groups that produce it to researchers elsewhere that analyze it. In many cases, therefore, the 6-hourly or daily data is archived on a subset of vertical levels to reduce the amount of data archived. For example, examining the current CMIP5 archive of 6-hourly and daily data, it was found that the 6-hourly data was typically only available on 3 vertical levels, obviously inadequate for moisture budget evaluation, and that daily data was available typically on 8 vertical levels. Hence we next determined how closely an evaluation with daily data on 8 levels can match the actual convergence of vertically integrated moisture, i.e. the comparison:

$$\overline{\overline{MC}} \quad c.f. \quad -\frac{1}{g\rho_w}\nabla_f \cdot \sum_{k=1}^{8} \overline{\overline{\mathbf{u}_{d,k} q_{d,k} \Delta p_{d,k}}}$$

This comparison already includes the error in going to daily or 6-hourly data and the error in going from 26 levels to 18 levels and then introduces an additional error in going to 8 levels from 18. However, we choose to show the total error in Figure 4. Comparing to the 18 level data, the 8 level case introduces significantly more error across the globe with notable errors appearing in the ITCZ regions and already existing errors over land becoming much larger.

The degradation of the balance in the moisture budget when reducing the vertical resolution to only 8 levels is really quite striking.

4) Error introduced by ignoring the sub-monthly variations of surface pressure

Up to now the vertical integrals have been performed at the temporal resolution of the data (e.g. each 6 hours or day) using the surface pressure at the same temporal resolution as the lower limit of integration. This allows for any co-variation between flow fields, specific humidity and surface pressure. However, it is our experience that high temporal resolution surface pressure data are not always available so next we address the error introduced by first computing the time mean of the covariance of $\mathbf{u}$ and q and then vertically integrating this using the time mean surface pressure. Introducing a single overbar to denote a monthly mean, we perform the comparisons:

$$
\begin{aligned}
-\frac{1}{g\rho_w}\nabla_f \cdot \sum_{k=1}^{K} \overline{\overline{\mathbf{u}_{6,k}q_{6,k}}\,\overline{\Delta p_{6,k}}} \quad c.f. \quad -\frac{1}{g\rho_w}\nabla_f \cdot \sum_{k=1}^{K} \overline{\overline{\mathbf{u}_{6,k}q_{6,k}\Delta p_{6,k}}} \\
-\frac{1}{g\rho_w}\nabla_f \cdot \sum_{k=1}^{K} \overline{\overline{\mathbf{u}_{d,k}q_{d,k}}\,\overline{\Delta p_{d,k}}} \quad c.f. \quad -\frac{1}{g\rho_w}\nabla_f \cdot \sum_{k=1}^{K} \overline{\overline{\mathbf{u}_{d,k}q_{d,k}\Delta p_{d,k}}}
\end{aligned}
$$

Figure 5 shows this comparison with daily data for both the 18 and 26 layer versions and with 6-hourly data for 26 layers. In no case are there important increases in error when going from daily vertical integrals to calculations that use monthly mean flow-humidity covariances together with monthly mean pressure thicknesses (see also Table 2). These comparisons show that no significant additional error is introduced by first time averaging the covariance of $\mathbf{u}$ and q and then vertically integrating this using the time mean p_s as the lower limit of integration.

5. Breaking down the moisture budget into components related to divergent flow, mean flow advection of moisture and transient eddy fluxes

The form of the moisture budget equation examined so far is quite useful and would allow a break down of, say, $P-E$ anomalies (or change) into components due to circulation and humidity anomalies (or change) since either $\mathbf{u}$ or q can be held at climatological values while the other one is allowed to vary, all within the vertical integral and the divergence operator (see below). However, this form does not allow an assessment of the relative roles of divergent circulations (i.e. the $q\nabla\cdot\mathbf{u}$ term) and advection of moisture (i.e. the $\mathbf{u}\cdot\nabla q$ term) to $P-E$. In order to assess that, we must return to a form with the divergence operator inside the vertical integral which then introduces the surface boundary term as in Eqs. 14 and 15. The problem then emerges when trying to evaluate the $\int_0^{p_s}\nabla\cdot(\mathbf{u}q)dp$ term because, in the presence of varying surface pressure, the lower limit of integration is different at the grid points used to perform the divergence operator. For example is the right approach to evaluate $\nabla\cdot(\mathbf{u}q)\approx\nabla_f\cdot(\mathbf{u}q)$ only at the pressure levels that exist for all the points used in the divergence operator (Eq. 15), $(i+1,j),(i-1,j),(i,j+1),(i,j-1)$, or is the right approach to also incorporate grid points that are at pressure levels which are nonexistent (higher pressure than surface pressure) and assume that $\mathbf{u}$ is zero at those points? And, in either case, how is the surface boundary term to be evaluated?

Fortunately there is a way to do this that yields the correct answer. To illustrate the approach we will reduce the problem to (x,p) dimensions and examine:

$$\frac{\partial}{\partial x}\left(\int_0^{p_s}(uq)dp\right)=\int_0^{p_s}\frac{\partial(uq)}{\partial x}dp+u_sq_s\frac{\partial p_s}{\partial x} \tag{21}$$

where $x=a\lambda\cos\phi$ and require that the numerical methods chosen to evaluate these terms ensure a balance.

Referring to Figure 6, and temporarily reintroducing i subscripts on K, we use K_i to indicate the lowest pressure level at grid point i that is above the surface, i.e. has a pressure, p_{K_i} lower than the surface pressure at the grid point, p_{s_i}. Then Eq. 21, evaluated between grid points i and $i+1$, is approximated by:

$$\left[\frac{\partial}{\partial x}\left(\int_0^{p_s}(uq)dp\right)\right]_{i+1/2} \approx \frac{1}{x_{i+1}-x_i}\left\{\sum_{k=1}^{K_{i+1}}(uq)_{i+1,k}\Delta p_k + (uq)_{i+1,K_{i+1}}\left(p_{s,i+1}-p_{K+1/2}\right) - \left[\sum_{k=1}^{K_i}(uq)_{i,k}\Delta p_k + (uq)_{i,K_i}\left(p_{s,i}-p_{K+1/2}\right)\right]\right\}. \quad (22)$$

Here, for example, at a latitude ϕ, $x_i = a\cos\phi\lambda_i$ Next we let the level $k = kk$ equal the lowest level with pressure $p = p_{kk}$ for which all the adjacent grid points have $p_s \geq p_{kk}$. Then Eq. 22 can be rewritten as:

$$\left[\frac{\partial}{\partial x}\left(\int_0^{p_s}(uq)dp\right)\right]_{i+1/2} \approx \frac{1}{x_{i+1}-x_i}\left\{\sum_{k=1}^{kk}\left[(uq)_{i+1,k}-(uq)_{i,k}\right]\Delta p_k + \sum_{k=kk+1}^{K_{i+1}}(uq)_{i+1,k}\Delta p_k - \sum_{k=kk+1}^{K_i}(uq)_{i,k}\Delta p_k + (uq)_{i+1,K_{i+1}}\left(p_{s,i+1}-p_{K+1/2}\right) - (uq)_{i,K_i}\left(p_{s,i}-p_{K+1/2}\right)\right\} \quad (23)$$

where it is understood that the sum $\sum_{k=kk+1}^{K}$ is only performed for $K \geq kk+1$ which, by definition, means only at $i+1$ for surface height decreasing westward and i for surface height increasing westward.

The first right hand side term in Eq. 23 provides a straightforward approximation to the first right hand side term in Eq. 21 viz:

$$\left[\int_0^{p_s}\frac{\partial(uq)}{\partial x}dp\right]_{i+1/2} \approx \sum_{k=1}^{kk}\frac{(uq)_{i+1,k}-(uq)_{i,k}}{x_{i+1}-x_i}\Delta p_k \quad (24)$$

The remainder of Eq. 22 provides an approximation to the surface term in Eq. 20 as follows:

$$\left(u_s q_s\frac{\partial p_s}{\partial x}\right)_{i+1/2} = \frac{1}{x_{i+1}-x_i}\left\{\sum_{k=kk+1}^{K_{i+1}}(uq)_{i+1,k}\Delta p_k - \sum_{k=kk+1}^{K_i}(uq)_{i,k}\Delta p_k + (uq)_{i+1,K_{i+1}}\left(p_{s,i+1}-p_{K+1/2}\right) - (uq)_{i,K_i}\left(p_{s,i}-p_{K+1/2}\right)\right\} \quad (25)$$

We refer to this surface term as SFC_K. The fact that this approximation holds can be seen by supposing the special case when uq is uniform everywhere and hence equals $(u_s q_s)_{i+1/2}$ in which case Eq. 25 reduces to:

$$\left(u_s q_s \frac{\partial p_s}{\partial x}\right)_{i+1/2} = (u_s q_s)_{i+1/2} \frac{p_{s,i+1} - p_{s,i}}{x_{i+1} - x_i} \tag{26}$$

If the surface term is evaluated as in Eq. 25 and the vertical integral of the divergence of moisture as in Eq. 24 then the sum of these two terms will exactly equal that given by Eq. 22 (or 23) and the balance in Eq. 21 is assured. As such, since all the data needed to evaluate both Eq. 22 and 24 are typically available, we would recommend that the surface term be evaluated as the difference between these and avoid the need to explicitly calculate it from Eq. 25.

It should be noted that the surface term, despite not being easily interpreted in a physical way, is not small. In Figure 7 we show the annual mean climatological moisture budget terms. Comparison of the mean flow moisture convergence (top right) with the total moisture convergence (top left) shows how dominant the mean flow is in explaining the moisture budget while the differences show the importance of the transient eddies in the mid-latitudes and subtropics. Figure 7 also shows the vertical integral of moisture divergence (the two dimensional analog of Eq. 24) and the surface term (the two dimensional analog of Eq. 25, but evaluated as a residual between two dimensional analogs of Eqs. 23 (or 22) and 24). It is clear that, for the moisture transport by the mean flow, the pattern and amplitude is preserved whether the convergence is computed before or after the vertical integral is performed. However, it is also clear that the surface term, $\overline{\overline{SFC}}_K$, is large wherever there are large gradients of surface pressure such as at coasts (where altitude can change abruptly) and over mountain ranges and, hence, cannot be ignored in the moisture budget.

Bringing the divergence operator inside the vertical integral allows the moisture divergence term to be broken into components related to the divergent flow and to advection across humidity gradients as in Eq. 15. This is usually performed on the monthly mean fields. Denoting, once more, ERA-reported monthly means by a single overbar, in Figure 7 we also show climatological values of the terms in:

$$-\frac{1}{g\rho_w}\sum_{k=1}^{kk}\overline{\nabla_f\cdot(\overline{\mathbf{u}}_k\overline{q}_k)\,\overline{\Delta p}_k} = -\frac{1}{g\rho_w}\sum_{k=1}^{kk}\overline{(\overline{q}_k\nabla_f\cdot\overline{\mathbf{u}}_k)\,\overline{\Delta p}_k} - \frac{1}{g\rho_w}\sum_{k=1}^{kk}\overline{(\overline{\mathbf{u}}\cdot\nabla_f\overline{q}_k)\,\overline{\Delta p}_k} \quad (27)$$

The mass divergence is clearly the dominant term in explaining the pattern of the mean flow moisture divergence. However, the mean flow advection term acts to dry the tropics, where the trades flow from drier regions to moister regions, and moistens the mid-latitudes where the surface westerlies flow from moister regions to drier regions.

a. *Summary*

Table 2 provides a quantitative assessment of the sizes of the various sources of error. First of all we see that errors are much larger over land than ocean, presumably due to the complexity of three dimensional spatial structures of winds and humidity. Errors are also larger in the tropics than extra tropics but this follows from the moisture convergences and divergences being larger there. The increase in error going from 6 hourly to daily data is, however, concentrated in the extra tropics and is related to the transient eddy moisture transport. Errors due to reduced vertical resolution are not striking in going from 26 to 18 levels but are large over land and ocean, in the tropics and extra tropics, when going to only 8 levels (typical of CMIP archives of daily data). Using monthly mean flow-humidity covariances together with monthly mean pressure thicknesses is in all cases an acceptable approximation.

6. Errors in the evaluation of moisture budget anomalies: Case study of the 1993 Mississippi Valley flood

We have demonstrated the errors that are introduced into moisture budgets when evaluated diagnostically with archived data. However, that was done with climatological moisture budgets. Next we need to assess the errors involved when analyzing the moisture budget anomalies associated with certain events of interest such as floods and droughts. It is possible, after all, that the climatological errors are persistent enough in time that they do not appear within the anomalous budgets. To examine this we choose the case of the late spring-early summer 1993 Mississippi Valley flood which represents an extreme seasonal anomaly of $P-E$ sustained by anomalous moisture convergence.

The analysis was conducted with the 26 level and 6 hourly data but using integration down to the monthly mean (as opposed to daily) surface pressure since we showed in Section 4 that this approximation does not introduce important error. The equation we begin with is then:

$$\overline{(P-E)}_{der} = -\frac{1}{g\rho_w}\nabla_f \cdot \sum_{k=1}^{K} \overline{\mathbf{u}_{6,k}q_{6,k}}\,\overline{\Delta p_{6,k}} \tag{28}$$

Here, as before, the single overbar denotes monthly mean quantities and $\overline{(P-E)}_{der}$ indicates the $P-E$ implied by the evaluated moisture convergence (as opposed to that reported by ERA-I or implied by $\overline{MC}$). We are interested in evaluating this for the average of May, June and July 1993 (MJJ 1993) when the floods occurred and determining the anomalies relative to the climatological situation. With ERA-I we can evaluate the moisture convergence anomalies for MJJ 1993 directly from the reported values of MC and then we can also evaluate this from Eq. 28. Therefore, using the second overbar to denote the long term climatological monthly mean, and a hat above an overbar to denote a departure of a particular monthly mean from the climatological value, e.g. $\overline{q} = \overline{\overline{q}} + \hat{\overline{q}}$ we evaluate:

$$\widehat{\overline{MC}} = \overline{MC} - \overline{\overline{MC}} \tag{29}$$

$$\begin{aligned} -\frac{1}{g\rho_w}\nabla_f \cdot \sum_{k=1}^{K} \widehat{\overline{\mathbf{u}_{6,k}q_{6,k}}\,\overline{\Delta p_{6,k}}} &= -\frac{1}{g\rho_w}\nabla_f \cdot \sum_{k=1}^{K} \overline{\mathbf{u}_{6,k}q_{6,k}}\,\overline{\Delta p_{6,k}} \\ &\quad - \left(-\frac{1}{g\rho_w}\nabla_f \cdot \sum_{k=1}^{K} \overline{\overline{\overline{\mathbf{u}_{6,k}q_{6,k}}\;\overline{\Delta p_{6,k}}}}\right) \end{aligned} \tag{30}$$

In Figure 8 we show for MJJ 1993 (i.e. the average of the anomalies for the three months) the ERA-I reported vertically integrated moisture convergence anomaly, $\widehat{\overline{MC}}$, the estimate of this using 6-hourly archived data on 26 levels (i.e. the left hand side of Eq. 30), for both the globe and North America, the ERA-I reported $\widehat{\overline{P-E}}$ and the change of vertically integrated moisture across the three month period. Globally, there is a close level of agreement between the actual column integrated moisture convergence anomaly and that diagnostically calculated with the largest anomalies being moisture convergence over the central and western equatorial

Pacific and divergence to the north and south and within the Pacific ITCZ, consistent with outgoing long wave radiation anomalies at the time and related to a waning El Niño (e.g. Trenberth and Guillemot (1996)). Over North America the agreement is also good and shows a large and focused moisture convergence anomaly over the upper Mississippi Valley and a moisture divergence anomaly over most of the southern U.S. and the western Atlantic Ocean. The ERA-I reported $\widehat{\overline{P-E}}$ anomaly over North America agrees quite well with $\widehat{\overline{MC}}$. The change in moisture storage is small.

To assess the level of agreement between the actual and diagnostically computed anomalies, in Figure 9 we show the differences between ERA-I reported and diagnostically computed column integrated moisture convergence for MJJ 1993 and, for comparison, the climatological MJJ. The climatological error in MJJ is similar in character to that in the other seasons (Figure 1) and is noisy and not systematic over North America. The MJJ 1993 error is also not systematic and also smaller than the climatological difference. This means that the anomalous moisture convergence in any one month or season or, presumably, year can indeed be estimated in a useful way by the diagnostic computation. That this is so allows further analysis of dynamical and thermodynamical causes of the anomalies of interest.

To determine causes of $P-E$ anomalies we break down the moisture convergence anomaly into components due to mean circulation anomalies, mean humidity anomalies and transient eddy moisture flux anomalies. To do this we first note that 6-hourly quantities are given, e.g. for q_6, by:

$$q_6 = \overline{q} + q_6' = \overline{\overline{q}} + \hat{\overline{q}} + q_6', \tag{31}$$

where the prime denotes a departure of 6-hourly data from the monthly mean (which itself equals the climatological monthly mean plus the monthly mean anomaly). Substituting expansions like Eq. 31 into Eq. 28 we can derive equations for the monthly mean climatology and anomalies in $\overline{(P-E)}_{der}$ or, equivalently, the diagnostically computed moisture convergence, in terms of components of the flow and humidity fields:

$$\overline{\overline{(P-E)}}_{der} \approx -\frac{1}{g\rho_w}\nabla_f \cdot \sum_{k=1}^{K}\left(\overline{\overline{\mathbf{u}_k}}\,\overline{\overline{q_k}} + \overline{\overline{u'_{6,k}q'_{6,k}}}\right)\overline{\overline{\Delta p_k}} \tag{32}$$

$$(\widehat{\overline{P-E}})_{der} \approx -\frac{1}{g\rho_w}\nabla_f \cdot \sum_{k=1}^{K}\left(\widehat{\overline{\mathbf{u}}_k\overline{q}_k\overline{\Delta p_k}} + \overline{\widehat{\mathbf{u}'_{6,k}q'_{6,k}}\,\Delta p_k}\right), \tag{33}$$

$$\approx -\frac{1}{g\rho_w}\nabla_f \cdot \sum_{k=1}^{K}\left(\overline{\overline{\mathbf{u}}}_k\hat{\overline{q}}_k + \hat{\overline{\mathbf{u}}}_k\overline{\overline{q}}_k + \widehat{\overline{\mathbf{u}'_{6,k}q'_{6,k}}}\right)\overline{\overline{\Delta p_k}}, \tag{34}$$

where, to derive the approximation in Eq. 34, products of monthly anomalies and terms involving $\widehat{\overline{\Delta p_k}}$ have been neglected. (It was found that, in general, ignoring the surface pressure variations which dictate variations in $\widehat{\overline{\Delta p_k}}$ introduces little additional error. Further, in the case of Eq. 34, which combines terms that are climatological and terms that are monthly anomalies, it would be ambiguous what to use for $\widehat{\overline{\Delta p_k}}$ and, hence, using climatological values seems expedient[1].) In Eq. 34 the first term on the right hand side is the anomaly in implied $P-E$ due to anomalies in mean specific humidity working with the climatological circulation, the second term is the anomaly due to the anomaly in mean circulation working with the climatological specific humidity and the third term is the anomaly due to anomalies in the moisture convergence by sub-monthly timescale transient eddies.

In Figure 10 we show the combined contribution of the mean flow and mean humidity to the moisture convergence anomaly and also the contribution from transient eddy moisture convergence, using now combinations of 18 and 26 levels and 6-hourly and daily data (i.e. the breakdown in Eq. 33). The mean flow and humidity anomalies caused the moisture convergence anomaly in the central U.S. and this is well approximated with only 18 levels. The contribution of mean flow moisture convergence to the floods is consistent with the persistently strong Great Plains Low Level Jet identified by Weaver et al. (2009). The transient eddy moisture convergence anomaly, in contrast, provides a north-south dipole with divergence over the southeastern U.S. and convergence to the north resulting in a shift northward of the total moisture convergence anomaly. The transient eddy moisture convergence anomaly

[1]In Seager et al. (2012) (see also Seager and Naik (2012)) anomalies in moisture budgets were examined using compositing over model El Niño and La Niña events and the pressure integrals were chosen to correspond to surface pressure anomalies during these events but the ambiguity introduced by breakdowns into terms combining climatological and anomaly quantities is not avoided.

evaluated with 6-hourly data is well approximated with 18 levels. The transient eddy moisture flux convergence pattern is consistent with the argument of Trenberth and Guillemot (1996) (based on flux anomalies but not on convergence) that the storm track anomalies in MJJ 1993 transfered moisture from the Gulf of Mexico into the upper Mississippi valley. When the transient eddy moisture convergence and divergence anomalies are evaluated with daily data the patterns are consistent with their 6-hourly counterparts but are notably weaker. As for the climatological case, it is clear that daily data is inadequate for evaluating transient eddy fluxes and divergence and that accuracy requires 6-hourly data.

The next step is to determine the relative contribution to the $P-E$ anomaly of changes in the mean flow and changes in the mean humidity, i.e. the breakdown in Eq. 34. In Fig. 11 we show the mean flow moisture convergence anomaly (repeated from Figure 10), together with the anomalous mean moisture flux vectors, and then the part of this that is caused by the flow anomalies combining with the climatological humidity field, and its associated vectors. The similarity of these two sets of fluxes and convergences indicates clearly that the circulation anomaly is the prime contributor to the $P-E$ anomaly while changes in humidity are less important (but not trivial). This result emphasizes the atmospherical dynamical origin of the MJJ 1993 flood in agreement with earlier studies (Mo et al. 1995; Liu et al. 1998). Figure 11 also shows the vectors of the transient eddy moisture flux together with their convergence (repeated from Figure 10) which reveal the northwestward flux of moisture by the eddies from the southeast U.S. towards the upper Mississippi Valley.

It is also of interest how the mean flow moisture convergence anomaly is contributed to by the divergent flow (and balancing vertical motion) and by moisture advection as in Eqs. 15 and 27. In this case we rewrite Eq. 33, with the help of Eqs. 14 and 15, and replacing the pressure thicknesses with climatological values, as:

$$(\widehat{\overline{P-E}})_{der} \approx -\frac{1}{g\rho_w}\sum_{k=1}^{K}\left(\overline{q}_k\widehat{\nabla_f \cdot \overline{\mathbf{u}}}_k + \overline{\mathbf{u}}_k \widehat{\cdot \nabla_f}\overline{q}_k\right)\overline{\overline{\Delta p_k}} - \frac{1}{g\rho_w}\nabla_f \cdot \sum_{k=1}^{K}\left(\widehat{\overline{\mathbf{u}'_{6,k}q'_{6,k}}}\right)\overline{\overline{\Delta p_k}} - \widehat{\overline{SFC}}_K. \tag{35}$$

To perform this breakdown the divergence operator has to be brought inside the vertical integration and hence the surface term, SFC_K, is reintroduced. Figure 12 shows this breakdown for MJJ 1993. In the left column we once more show the total anomalous convergence (mean plus transient flows) of vertically integrated moisture at the top (repeated from Figure 10) and below it the anomalous vertical integral of the total moisture convergence and the surface term, SFC_K. As for the climatological case (Figure 7), the pattern and amplitude of anomalous moisture convergence is preserved whether or not the convergence is performed before or after the vertical integral. However, as before, the surface term is non-negligible over the North American continent because of the presence of sizable surface pressure gradients. In the right column of Figure 12 we show the total anomalous *mean flow* moisture convergence once more and its breakdown into a part due to the divergent mean flow and a part due to mean flow advection across mean humidity gradients. Both terms are important with clear roles for the term involving the mean flow convergence and ascending air in the region of highest $P - E$ anomaly in the Mississippi Valley and for the moisture advection term further to the east. The advection term here includes the advection of the mean specific humidity field by the anomalous flow and, referring to Figure 11, the strong southerly component to the flow anomalies in MJJ 1993 would create a positive $P - E$ tendency in that way.

Finally for the analysis of the MJJ 1993 Mississippi Valley floods, we examine how well the anomalies would be captured if only 8 levels of daily data were available, as is common for CMIP archives of daily data. The 8 layer version quite reasonably captures the 26 level version of the total moisture convergence (Figure 13). The errors introduced are quite random spatially but, in general, are of the magnitude of the field itself.

In summary, with 6 hourly data and care and attention in the performance of divergence operators and vertical integrals, and their order of computation, the diagnosed moisture budget can be analyzed and broken down to yield important insights into the causes of major hydroclimate anomalies such as the MJJ 1993 Mississippi floods. Nonetheless, in this case of the MJJ 1993 floods, even an analysis of causes based on just 8 levels of daily data might lead to useful, if not definitive, results.

7. Conclusions

The ability to diagnose moisture budget variations, and their causes, within reanalyses and atmosphere models, using archived data has been evaluated. The work was performed using the ERA-I reanalysis data which reports vertically integrated moisture fluxes and convergences. This allows an assessment of errors introduced by diagnostically evaluating these terms from the archived data. The climatological moisture budget is evaluated as well as anomalies during the Mississippi Valley flood of May-June-July 1993. Due to the assimilation procedure the ERA-I does not have a closed moisture budget and precipitation minus evaporation, $P - E$, does not balance the vertically integrated moisture convergence and tendency. However, in diagnostic use of data from climate models, where this balance is more closely assured due to lack of data assimilation, the problem is always the evaluation of the vertically integrated moisture convergence. Hence here we focus on the evaluation of that using the ERA-I reanalysis as our test case. Conclusions are as follows:

- Estimating the ERA-I reported vertically integrated moisture convergence by applying a centered finite difference scheme to the ERA-I reported vertically integrated moisture fluxes introduces significant error which is greater over land than ocean. Errors are smaller when data closer to the ECMWF model resolution are used but do not disappear. The errors are probably partly due to the use of different numerical methods to evaluate the ERA-I reported convergence of vertically integrated moisture fluxes to those used in our diagnostic evaluation of moisture convergence. However, since the ECMWF model itself uses yet different methods to update its moisture field, and since the effects of moisture diffusion in the ERA-I cannot be diagnosed, some level of imbalance between diagnosed moisture convergence, $P - E$ and change in moisture storage has to be accepted.

- In mid-latitudes where transient eddies cause significant time-averaged covariances of flow and humidity and, hence, time averaged moisture fluxes and convergence, use of 6-hourly data introduces far less error than daily data. The error from using daily data appears as an underestimation of transient eddy moisture fluxes and convergence.

- Using 18 vertical levels instead of 26 vertical levels, with loss of vertical resolution in the boundary layer, introduces additional errors primarily over land areas and has little effect over the ocean presumably because of differences in the complexity of the vertical structure of winds and humidity. However, going from 18 levels to the 8 levels common in CMIP archives of daily data, introduces additional errors which are now spread across both land and ocean. Monthly mean data in CMIP archives is usually stored at greater vertical resolution. Calculating the mean flow moisture convergence at the higher resolution and the transient contribution at the reduced vertical resolution will reduce error.

- Daily surface pressure data is not always available in model archives. However, performing vertical integrals with monthly mean pressure fields does not cause a significant increase in error compared to performing vertical integrals each day with daily pressure fields or each 6 hours with 6-hourly pressure fields.

- When breaking down mean flow moisture convergence into components due to mass flux convergence and advection, the divergence operator has to be taken inside the vertical pressure integral which introduces a surface term, $q_s\mathbf{u}_s \cdot \nabla p_s$. A method is developed to numerically evaluate the vertical integral of mean flow moisture convergence and the surface term that assures that these sum exactly to equal the convergence of the vertically integrated moisture flux.

- Errors in diagnostically evaluating moisture budgets for particular seasons are no larger, and maybe smaller, than for climatological moisture budgets. This ensures that diagnosed moisture budgets can be reasonably examined to determine the causes of hydroclimate anomalies.

- The anomalous moisture budget evaluation was illustrated for the case of the Mississippi floods of May-June-July 1993. The diagnostically computed moisture convergence closely matches the ERA-I reported one as well as the ERA-I $P - E$. It is shown that mean flow moisture convergence related to a southerly flow anomaly and convergent flow was responsible for the positive $P - E$ in the central U.S. while an anomalous transient eddy moisture flux divergence dried the southeast U.S. and transient eddy moisture flux convergence moistened the upper Mississippi valley. It is also shown that the moisture budget anomalies responsible for the flood were largely caused by circulation anomalies combining with the mean flow with the impacts of humidity anomalies being weaker.

The contribution of the circulation anomalies was effected through both changes in mass convergence (and hence vertical motion) and changes in the advection of the mean humidity. The transient eddy contribution to the anomaly was underestimated with hourly data. However, an analysis with even 8 levels of daily data would reveal the major causes of the flood.

In this regard we make the following recommendation:

Recommendation: Climate models and reanalyses should compute covariances at the model time step and then average these into monthly means (e.g. archive monthly means of $\mathbf{u}_{T,k}q_{T,k}$, where T refers to time step values on the model vertical grid) for archiving in, for example, CMIP data and in Reanalysis data.

Monthly mean flow-humidity covariances can be vertically integrated with the monthly pressure fields to yield an accurate approximation to the total monthly mean convergence of vertically integrated moisture fluxes. With this saved, the transient contributions can be evaluated by subtracting the monthly mean contributions evaluated from the monthly mean data. Transient contributions estimated in this way will in fact be more accurate than those computed with archived 6-hourly data and even more accurate than those computed with daily data at the modest cost of increasing the size of model data archives. If this was done it would help researchers perform accurate analyses of the atmospheric branch of the hydrological cycle and further advance knowledge and prediction of the Earth's climate system.

Acknowledgments.

This work was supported by NOAA award NA10OAR4310137 (Global Decadal Hydroclimate Variability and Change). We would like to thank Yochanan Kushnir and Paul Berrisford (ECMWF) for useful discussions and Donna Lee for downloading the ERA-Interim data and the European Centre for Medium Range Weather Forecasts for making the reanalysis data available.

REFERENCES

Allen, M. R. and W. J. Ingram, 2002: Constraints on future changes in climate and the hydrologic cycle. *Nature*, **419**, 224–232.

Berrisford, P., P. Kallberg, S. Kobayashi, D. Dee, S. Uppala, A. J. Simmons, P. Poli, and H. Sato, 2011a: Atmospheric conservation properties in ERA-Interim. *Quart. J. Royal Meteor. Soc.*, **137**, 1381–1399.

Berrisford, P., et al., 2011b: The ERA-Interim archive version 2.0. Tech. rep., European Centre for Medium Range Weather Forecasts, ERA report series No. 1, 23 pp.

Cutter, S. L., C. T. Emrich, J. J. Webb, and D. Morath, 2009: Social Vulnerability to Climate Variability Hazards: A Review of the Literature. Tech. rep., Hazards and Vulnerability Research Institute, University of South Carolina, Columbia, SC, 44pp.

Dee, D., et al., 2011: The ERA-Interim Reanalysis; Configuration and performance of the data assimilation system. *Quart. J. Roy. Meteor. Soc.*, **137**, 553–597.

ECMWF, 2012: IFS Documentation Cy37r2 Operational implementation 18 May 2011. Part III: Dynamics and numerical procedures. Tech. rep., European Centre for Medium Range Weather Forecasts, 29 pp.

Harnik, N., R. Seager, N. Naik, M. Cane, and M. Ting, 2010: The role of linear wave refraction in the transient eddy-mean flow response to tropical Pacific SST anomalies. *Quart. J. Roy.Meteor. Soc.*, 2132-2146.

Held, I. M. and B. J. Soden, 2006: Robust responses of the hydrological cycle to global warming. *J. Climate*, **19**, 5686–5699.

Huang, H., R. Seager, and Y. Kushnir, 2005: The 1976/77 transition in precipitation over the Americas and the influence of tropical SST. *Clim. Dyn.*, **24**, 721–740.

Intergovernmental Panel on Climate Change, 2007: *Climate Change: The IPCC Scientific Assessment*. Cambridge University Press, Cambridge, England, 365 pp.

Konor, C. S. and A. Arakawa, 1997: Design of an atmospheric model based on a generalized vertical coordinate. *Mon. Wea. Rev.*, **125**, 1649–1673.

Liu, A. Z., M. Ting, and H. Wang, 1998: Maintenance of circulation anomalies during the 1988 drought and 1993 floods over the United States. *J. Atmos. Sci.*, **55**, 2810–2832.

Mo, K. C., J. Nogues-Paegle, and J. Paegle, 1995: Physical mechanisms of the 1993 summer floods. *J. Atmos. Sci.*, **52**, 879–895.

Nakamura, J., U. Lall, Y. Kushnir, A. W. Robertson, and R. Seager, 2012: Dynamical structure of major spring floods in the U.S. Midwest. *J. Hydromet.*, in press.

Seager, R., N. Harnik, W. A. Robinson, Y. Kushnir, M. Ting, H. P. Huang, and J. Velez, 2005: Mechanisms of ENSO-forcing of hemispherically symmetric precipitation variability. *Quart. J. Roy. Meteor. Soc.*, **131**, 1501–1527.

Seager, R. and N. Naik, 2012: A mechanisms-based approach to detecting recent anthropogenic hydroclimate change. *J. Climate*, **25**, 236–261.

Seager, R., N. Naik, M. A. Cane, N. Harnik, M. Ting, and Y. Kushnir, 2010a: Adjustment of the atmospheric circulation to tropical Pacific SST anomalies: Variability of transient eddy propagation in the Pacific-North America sector. *Quart. J. Roy. Meterorol. Soc.*, **136**, 277–296.

Seager, R., N. Naik, and G. A. Vecchi, 2010b: Thermodynamic and dynamic mechanisms for large-scale changes in the hydrological cycle in response to global warming. *J. Climate*, **23**, 4651–4668.

Seager, R., N. Naik, and L. Vogel, 2012: Does global warming cause intensified interannual hydroclimate variability? *J. Climate*, **25**, 3355–3372.

Seager, R. and G. A. Vecchi, 2010: Greenhouse warming and the 21st Century hydroclimate of southwestern North America. *Proc. Nat. Acad. Sci.*, **107**, 21 277–21 282.

Seager, R., et al., 2007: Model projections of an imminent transition to a more arid climate in southwestern North America. *Science*, **316**, 1181–1184.

Seneviratne, S. I., P. Viterbo, D. Luthi, and C. Schar, 2004: Inferring changes in terrestrial water storage using ERA-40 reanalysis data: The Mississippi River basin. *J. Climate*, **17**, 2039–2057.

Taylor, K. E., R. J. Stouffer, and G. A. Meehl, 2012: An Overview Of CMIP5 And The Experiment Design. *Bulletin of the American Meteorological Society*, **93 (4)**, 485–498.

Trenberth, K., 1997: Using atmospheric budgets as a constraint on surface fluxes. *J. Climate*, **10**, 2796–2809.

Trenberth, K., J. T. Fasullo, and J. Mackaro, 2011: Atmospheric moisture transport from ocean to land and global energy flows in Reanalyses. *J. Climate*, **24**, 4907–4924.

Trenberth, K. and C. J. Guillemot, 1995: Evaluation of the global atmospheric moisture budget as seen from analyses. *J. Climate*, **8**, 2255–2272.

Trenberth, K. and C. J. Guillemot, 1996: Physical processes involved in the 1988 drought and 1993 floods in North America. *J. Climate*, **9**, 1288–1298.

Trenberth, K. and C. J. Guillemot, 1998: Evaluation of the atmospheric moisture and hydrological cycle in the NCEP/NCAR reanalyses. *Clim. Dyn.*, **14**, 213–231.

Weaver, S. J., A. Ruiz-Barradas, and S. Nigam, 2009: Pentad evolution of the 1988 drought and 1993 flood over the Great Plains: An NARR perspective on the atmospheric and terrestrial water balance. *J. Climate.*, **22**, 5366–5384.

TABLE 1. The long term average of root mean square differences (mm/day) between the monthly mean diagnostically computed convergence of ERA-I reported vertically integrated moisture flux ($\nabla_f \cdot VIMF$) and, left column, the ERA-I reported monthly mean vertically integrated moisture convergence (MC) and, right columns, diagnostically computed convergences of diagnostically computed monthly mean vertical moisture fluxes.

$$rms\,(\,(\cdot)\;-\nabla_f\cdot\mathrm{VIMF})$$

	MC	6 hourly, 26 levels	6 hourly, 18 levels	6 hourly, 8 levels
Global	1.31	0.93	1.04	1.89
Land	1.94	1.34	1.53	2.82
Ocean	0.95	0.70	0.76	1.35
30°S-30°N	1.21	0.86	0.94	1.71
30°-90°	0.53	0.45	0.47	0.77

TABLE 2. The long term average of root mean square differences (mm/day) between monthly mean diagnostically computed divergence of vertically integrated moisture content and the ERA-I reported values of the same ($\overline{MC}$) for various combinations of vertical and time resolution of the diagnostic computations. Legend in the table corresponds to the usage in the main text except that n generically refers to the time resolution, either 6 hourly or daily.

Errors (mm/day)

	26 levels			18 levels			8 levels		
	$\overline{\overline{\mathbf{u}_n q_n \Delta p_n}}$	$\overline{\overline{\mathbf{u}_n q_n}\,\overline{\Delta p}}$	$\overline{\overline{\mathbf{u}_n q_n}}\,\overline{\overline{\Delta p}}$	$\overline{\overline{\mathbf{u}_n q_n \Delta p_n}}$	$\overline{\overline{\mathbf{u}_n q_n}\,\overline{\Delta p}}$	$\overline{\overline{\mathbf{u}_n q_n}}\,\overline{\overline{\Delta p}}$	$\overline{\overline{\mathbf{u}_n q_n \Delta p_n}}$	$\overline{\overline{\mathbf{u}_n q_n}\,\overline{\Delta p}}$	$\overline{\overline{\mathbf{u}_n q_n}}\,\overline{\overline{\Delta p}}$
6 hour									
Global	1.10	1.11	1.11	1.20	1.21	1.22	1.97	2.02	2.07
Land	1.57	1.57	1.57	1.74	1.76	1.79	2.90	3.00	3.08
Ocean	0.85	0.85	0.85	0.89	0.90	0.90	1.43	1.46	1.49
$\leq 30°$	1.06	1.06	1.06	1.12	1.12	1.12	1.81	1.83	1.86
30°-90°	0.52	0.52	0.52	0.54	0.55	0.56	0.82	0.86	0.91
daily									
Global	1.14	1.14	1.14	1.23	1.24	1.26	1.99	2.04	2.09
Land	1.58	1.59	1.59	1.76	1.78	1.80	2.91	2.99	3.07
Ocean	0.89	0.89	0.90	0.94	0.94	0.95	1.47	1.49	1.52
$\leq 30°$	1.07	1.07	1.07	1.13	1.13	1.13	1.82	1.84	1.86
30°-90°	0.64	0.64	0.64	0.66	0.67	0.68	0.93	0.97	1.01

List of Figures

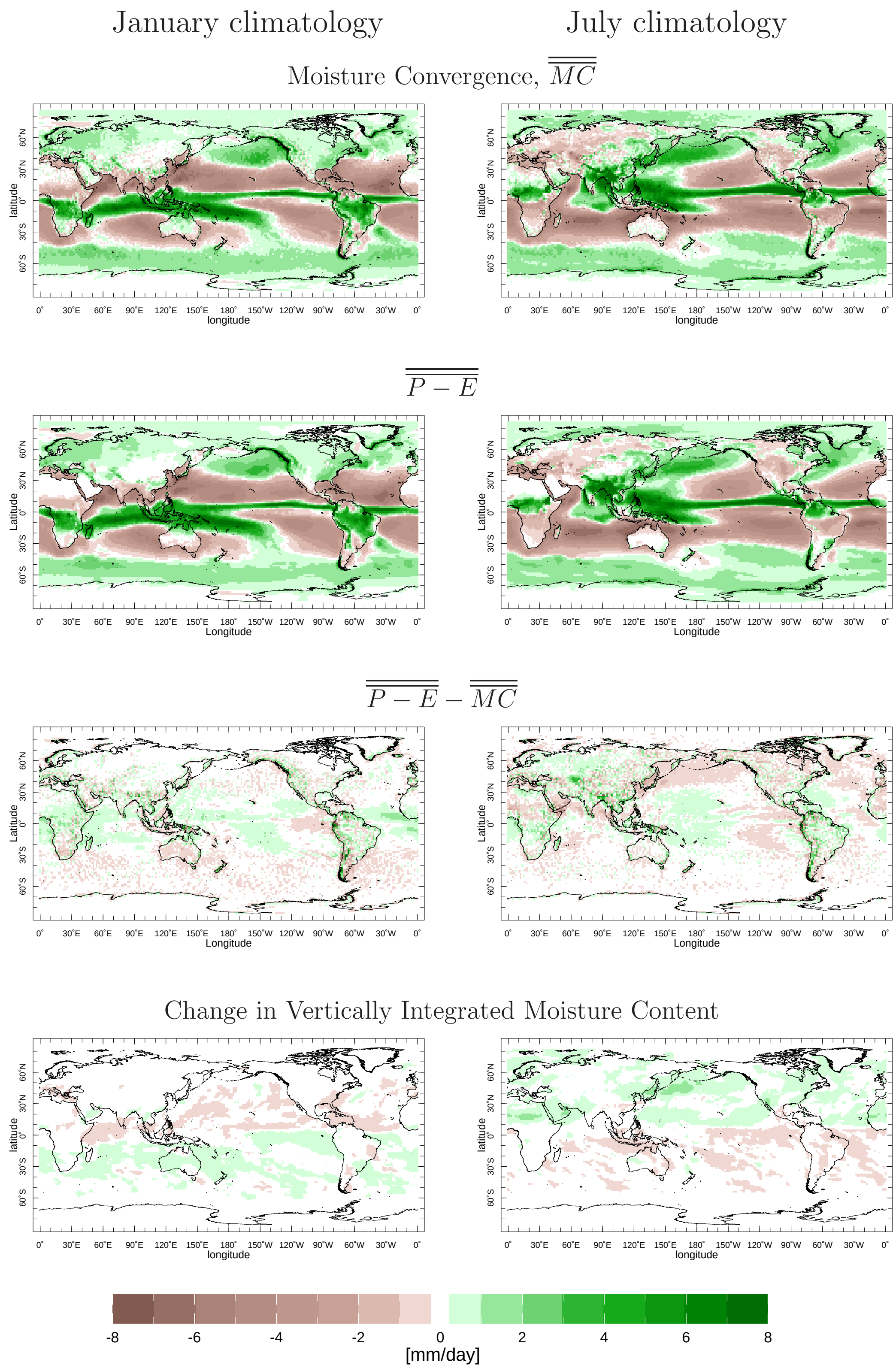

FIG. 1. The January (left column) and July (right column) climatologies of the ERA-Interim reported 'vertically-integrated moisture divergence', $\overline{\overline{MC}}$ (top), $\overline{\overline{P-E}}$ (upper middle), their difference (lower middle) and the change in moisture storage computed from the reported vertically integrated moisture content (bottom). Units are mm/day

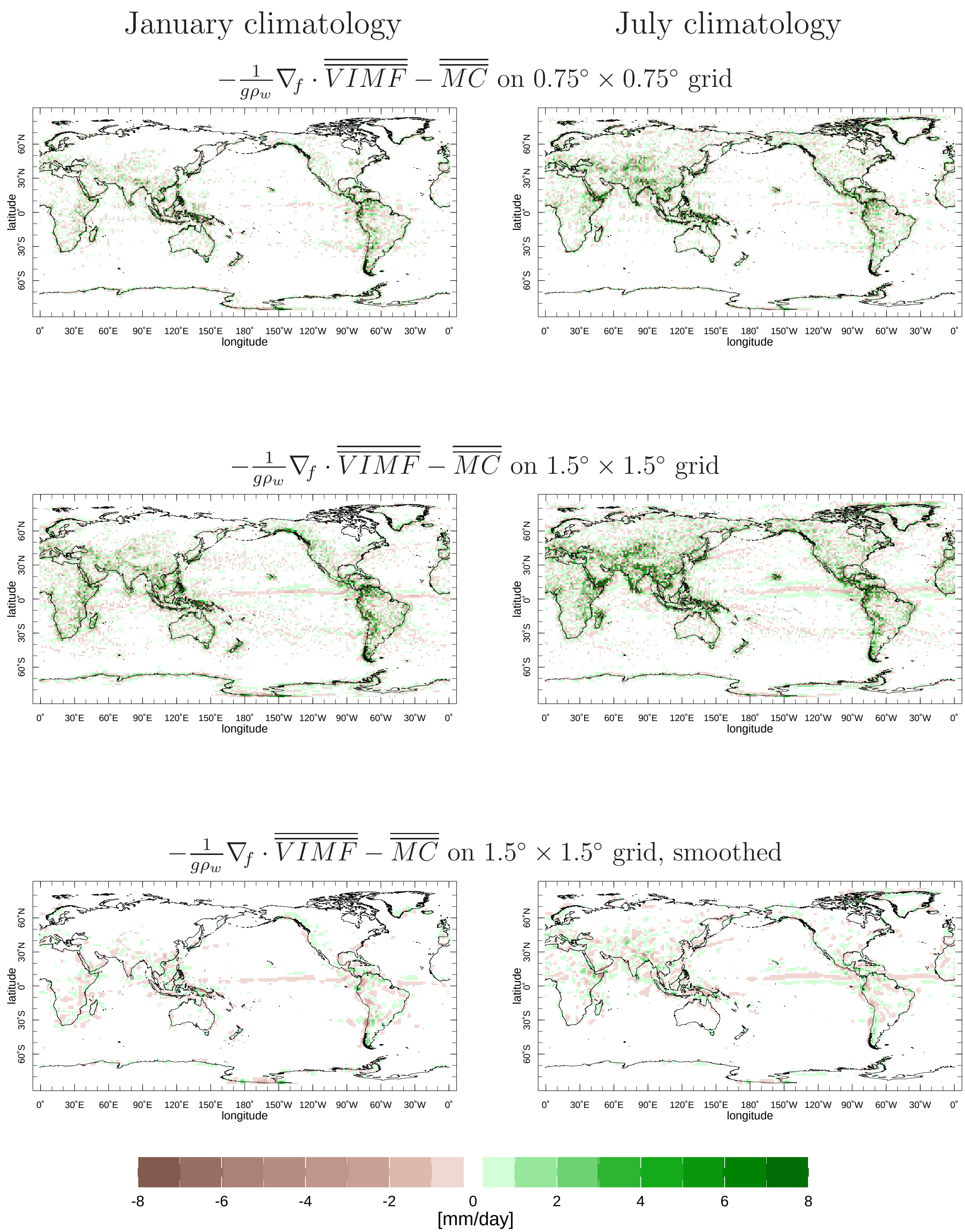

FIG. 2. The January (left column) and July (right column) climatologies of (top) the difference between the divergence of the ERA-Interim reported 'vertically-integrated moisture flux', $\overline{\overline{VIMF}}$ as evaluated using a centered finite difference scheme and the ERA-Interim reported value $\overline{\overline{\nabla_f \cdot VIMF}} - \overline{\overline{MC}}$ all on 1.5 degree grid and (middle) same as top but on a 0.75 degree grid and (bottom) same as top after application of one pass of a 1-2-1 spatial smoother. Units are mm/day

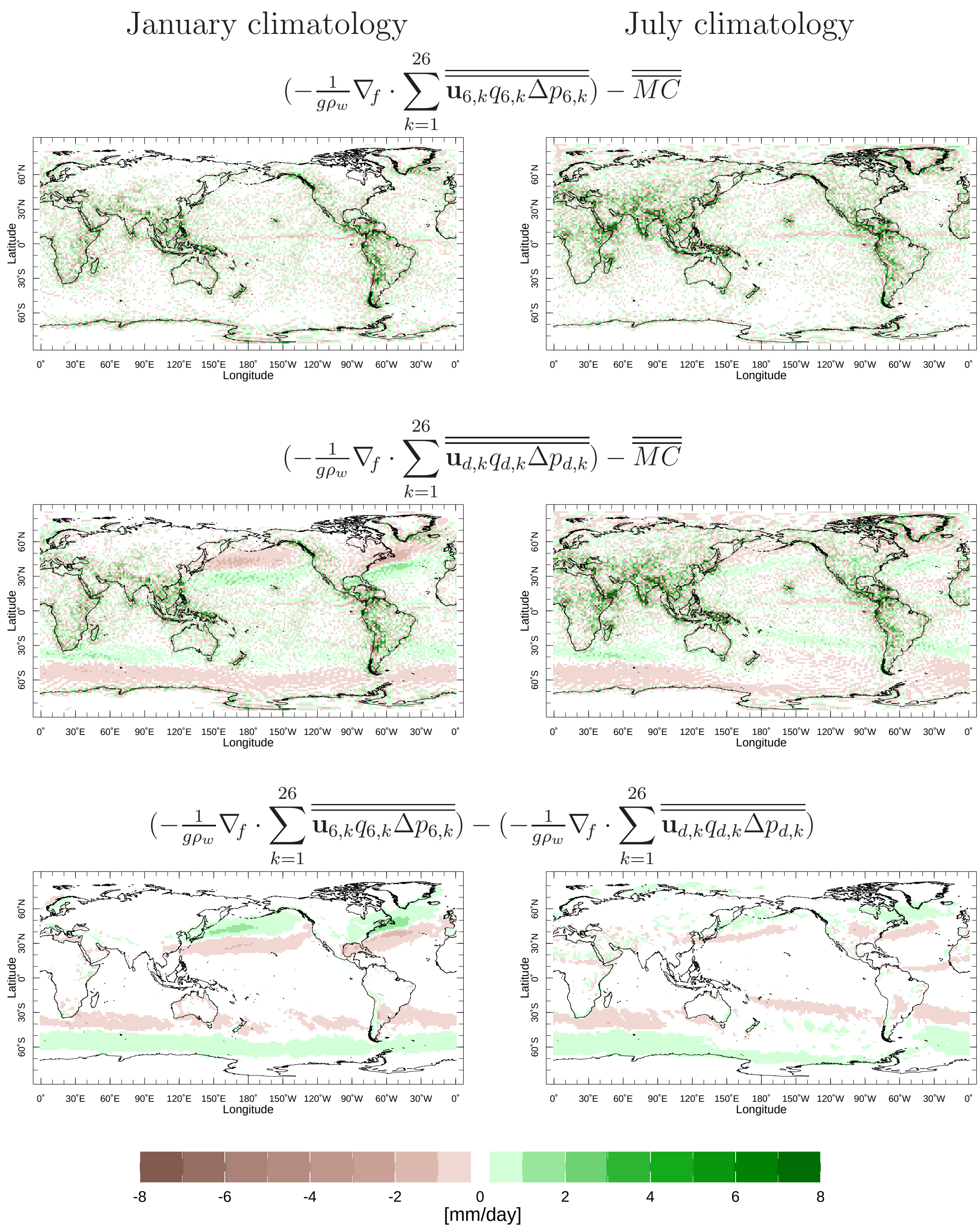

FIG. 3. The January (left column) and July (right column) climatological differences between the ERA-I reported vertically-integrated moisture convergence $\overline{\overline{MC}}$ (top) and that evaluated using archived 6-hourly data on 26 pressure levels (top), daily data on 26 pressure levels (middle) and the difference between 6-hourly and daily evaluations (bottom). Units are mm/day

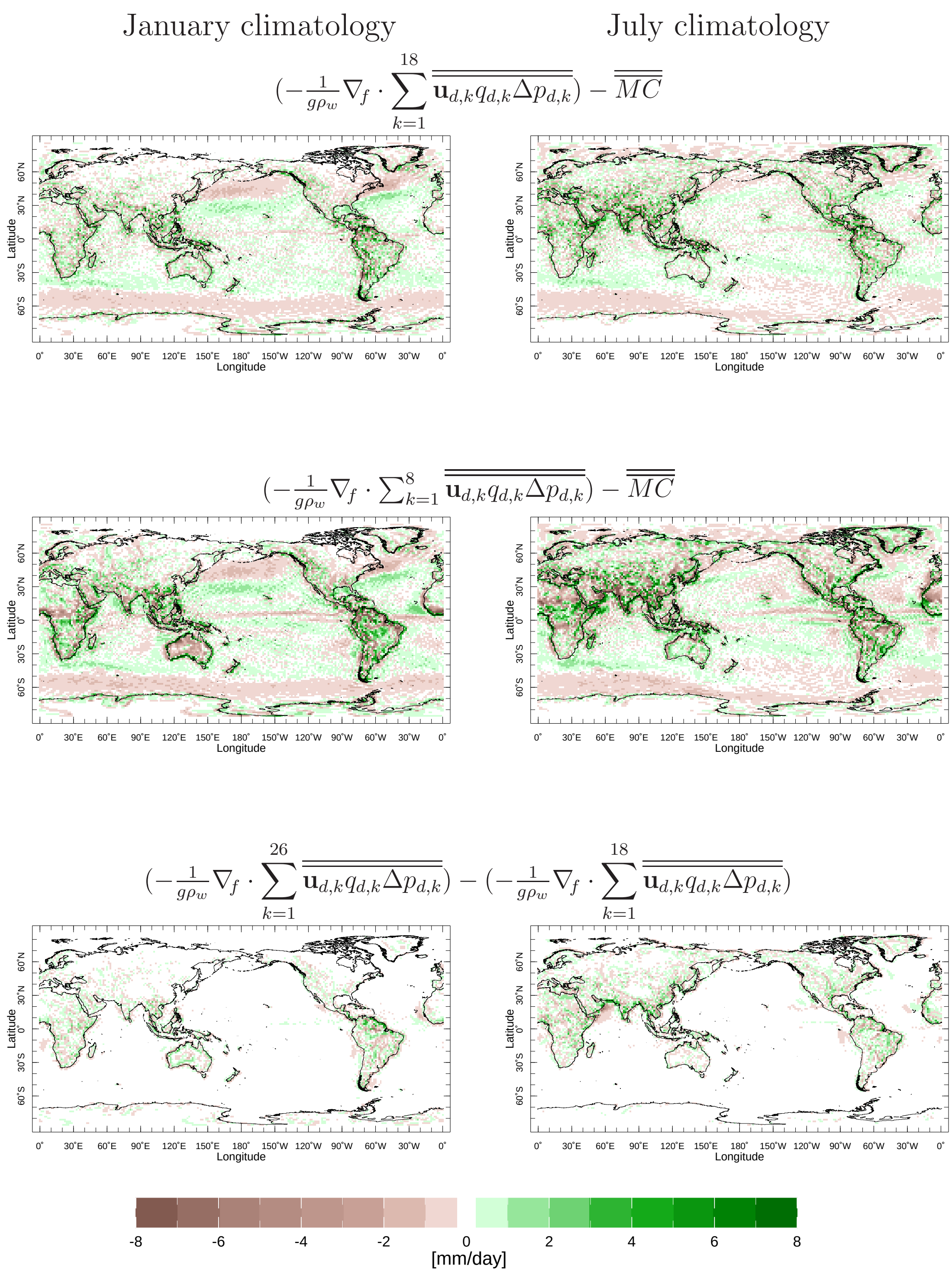

FIG. 4. The January (left column) and July (right column) climatological differences between the ERA-I reported vertically-integrated moisture convergence $\overline{\overline{MC}}$ (top) and that evaluated using archived daily data on 18 pressure levels (top), 8 pressure levels (middle) and the difference between evaluations using daily data and 26 levels versus 18 levels (bottom). Units are mm/day

January climatology | July climatology

$$\left(-\frac{1}{g\rho_w}\nabla_f\cdot\sum_{k=1}^{18}\overline{\overline{\mathbf{u}_{d,k}q_{d,k}}\,\overline{\Delta p_k}}\right)-\left(-\frac{1}{g\rho_w}\nabla_f\cdot\sum_{k=1}^{18}\overline{\overline{\mathbf{u}_{d,k}q_{d,k}\Delta p_{d,k}}}\right)$$

$$\left(-\frac{1}{g\rho_w}\nabla_f\cdot\sum_{k=1}^{26}\overline{\overline{\mathbf{u}_{d,k}q_{d,k}}\,\overline{\Delta p_k}}\right)-\left(-\frac{1}{g\rho_w}\nabla_f\cdot\sum_{k=1}^{26}\overline{\overline{\mathbf{u}_{d,k}q_{d,k}\Delta p_{d,k}}}\right)$$

$$\left(-\frac{1}{g\rho_w}\nabla_f\cdot\sum_{k=1}^{26}\overline{\overline{\mathbf{u}_{6,k}q_{6,k}}\,\overline{\Delta p_k}}\right)-\left(-\frac{1}{g\rho_w}\nabla_f\cdot\sum_{k=1}^{26}\overline{\overline{\mathbf{u}_{6,k}q_{6,k}\Delta p_{6,k}}}\right)$$

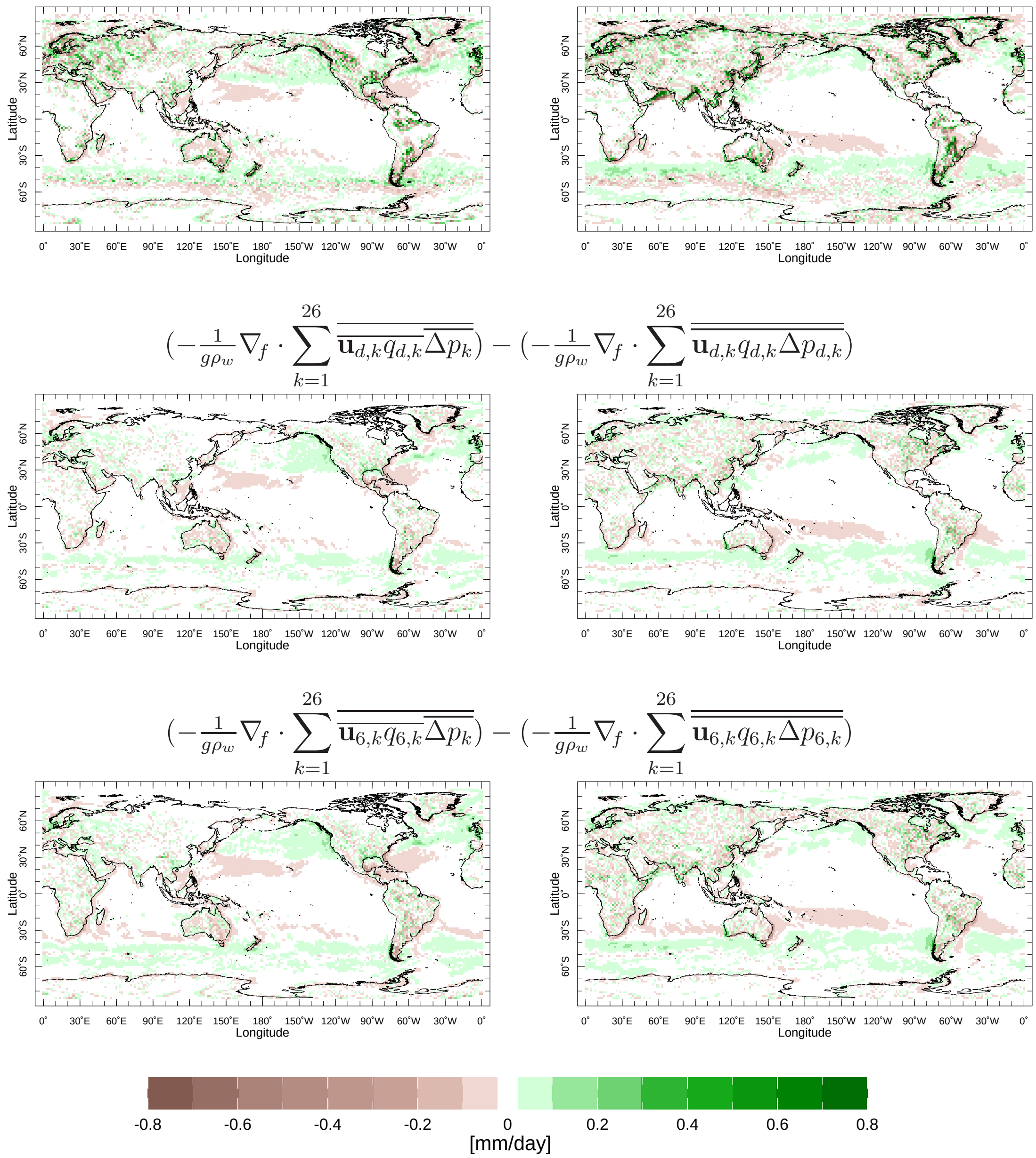

FIG. 5. The January (left column) and July (right column) climatological differences between evaluations of the convergence of vertically integrated moisture for the cases of using monthly means of daily wind and humidity covariances combined with monthly mean pressure thicknesses and the case that allows for daily covariances of wind, humidity and pressure thicknesses with 18 pressure levels (top), 26 pressure levels (bottom) and the same difference using 26 pressure levels (bottom). Units are mm/day

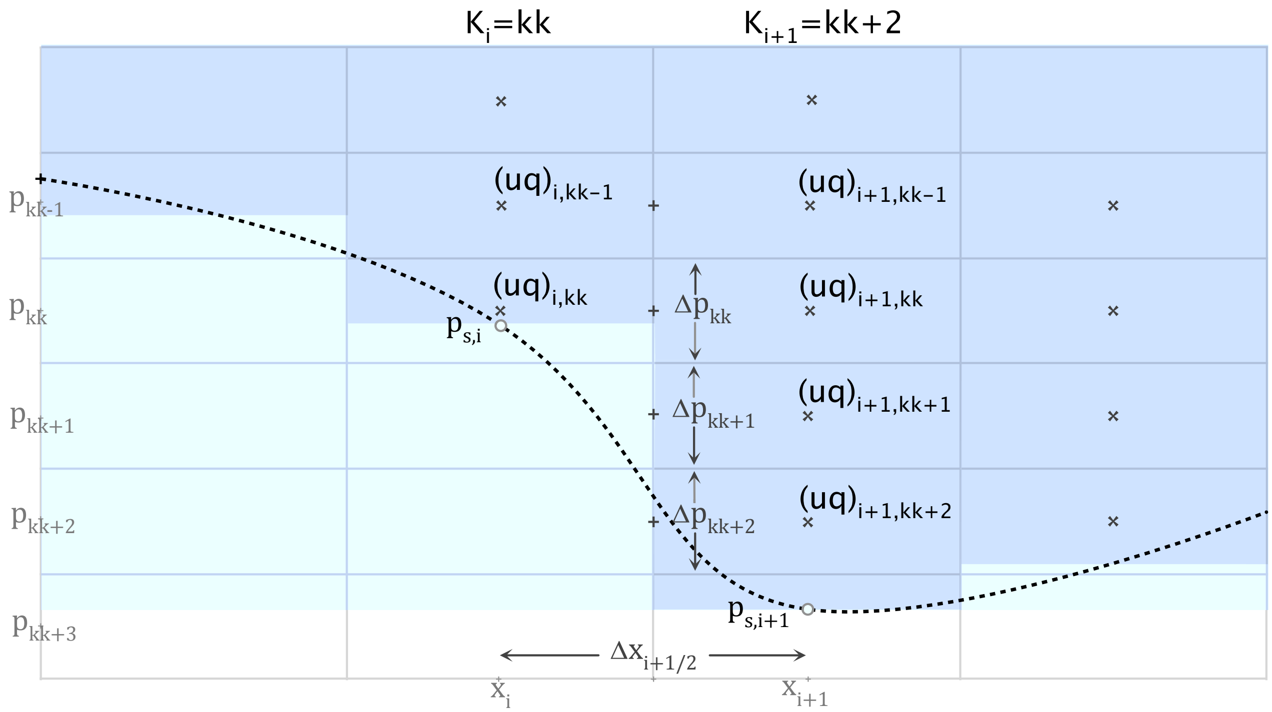

FIG. 6. Schematic of a pressure grid over uneven topography for reference in discussion of how to evaluate the surface term that appears when evaluating vertical integrals of moisture divergence, i.e. when the divergence operator is inside the vertical integral over pressure. K_i and K_{I+1} indicate number of vertical pressure levels at columns i and $i+1$, kk indicates the lowest level for which the the pressure, p_k is lower than the surface pressure at both grid points, i and $i+1$, needed to evaluate the divergence operator at $i+1/2$.

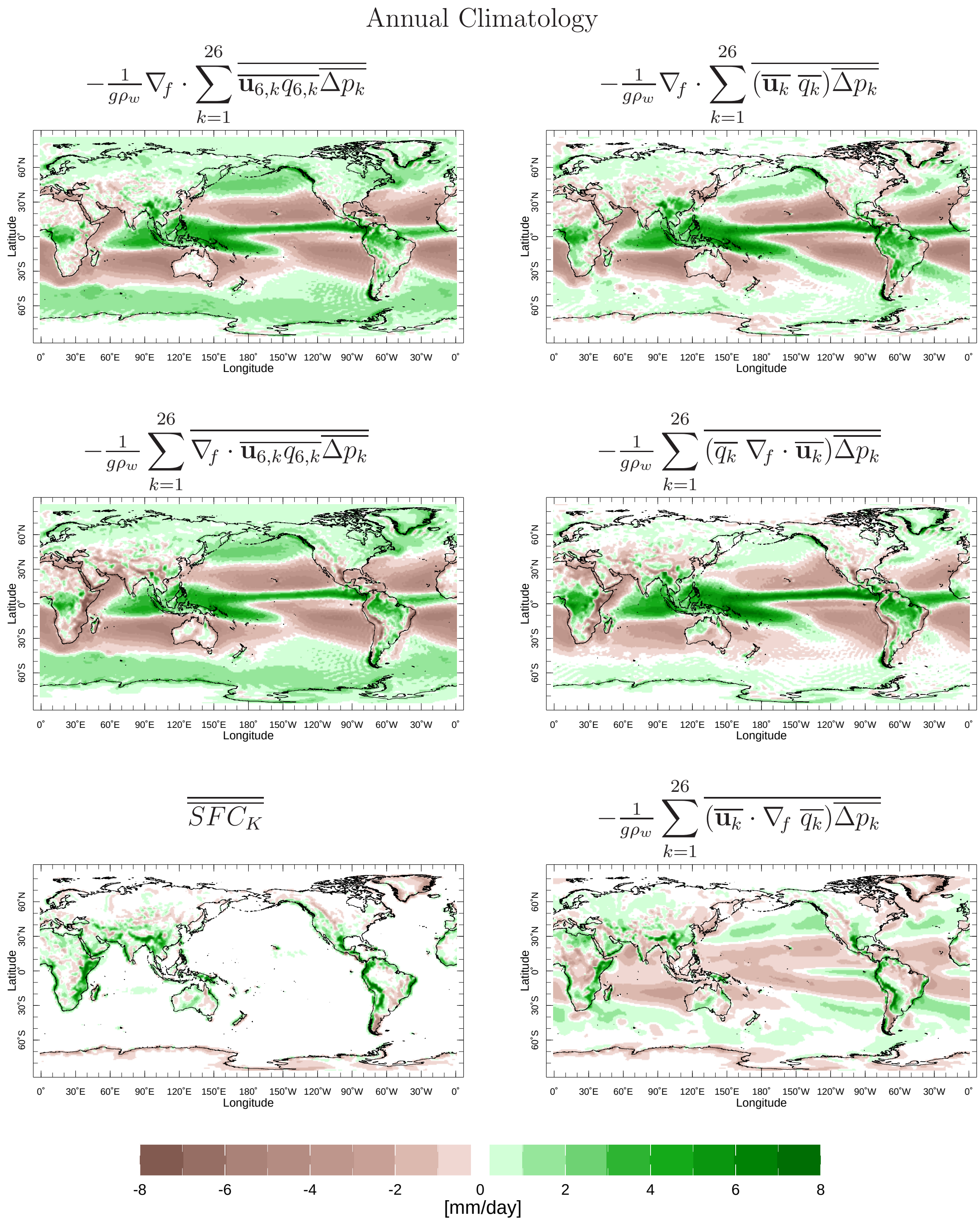

FIG. 7. The annual mean climatology of the convergence of vertically integrated total moisture flux (top left) and its two components, the vertical integral of total moisture convergence (middle left) and the total surface term (bottom left). The convergence of vertically integrated mean flow moisture flux (top right) is split into components due to the convergence mean flow (middle right) and mean flow advection (bottom right). Units are mm/day

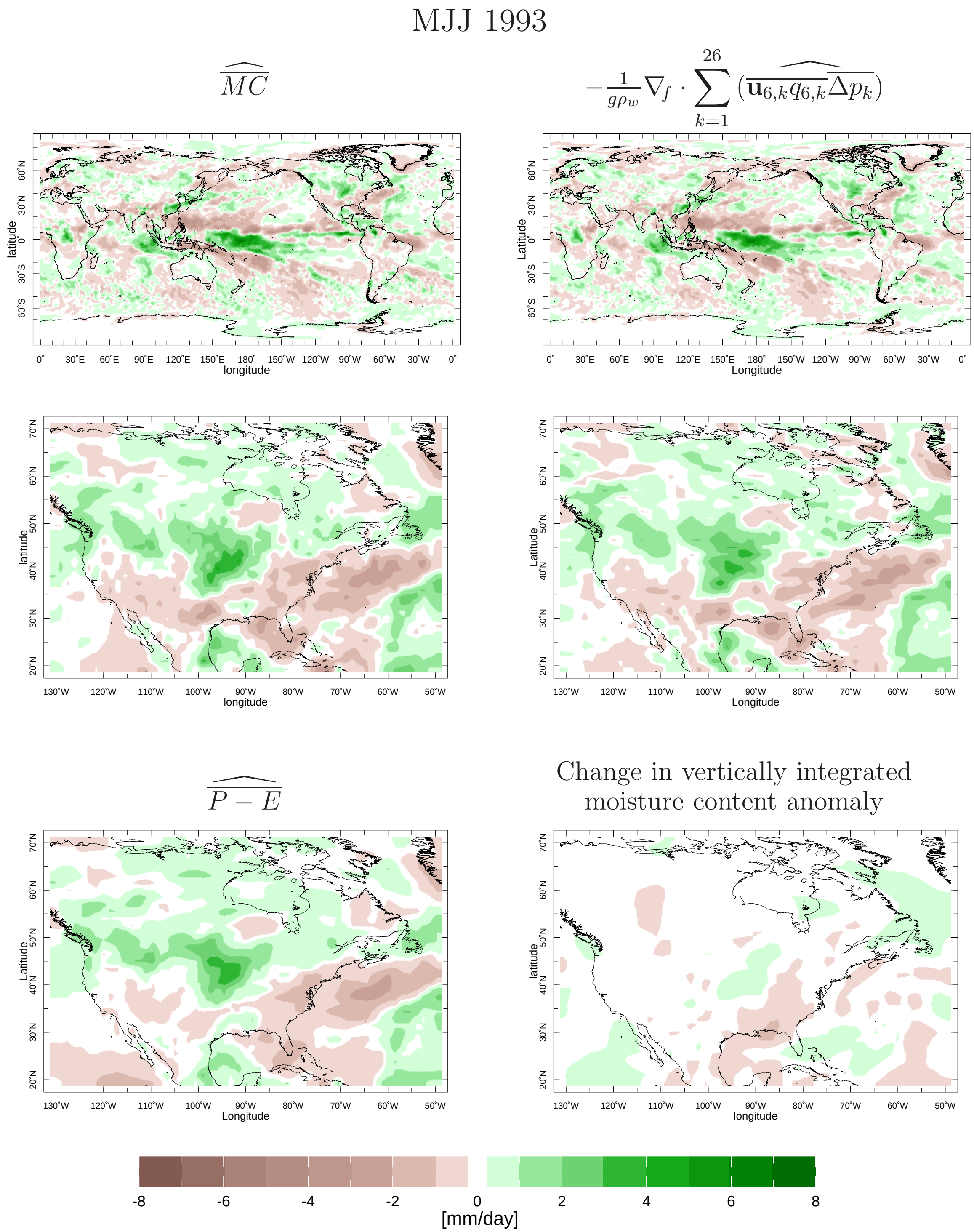

FIG. 8. The ERA-Interim reported (top and middle left) vertically integrated moisture convergence anomaly, and that computed diagnostically from 6 hourly data on 26 levels (top and middle right) for May-June-July 1993 for the globe (top) and North America (middle). At lower left the ERA-I reported $\widehat{P-E}$ is shown and at bottom right the change in moisture storage.Units are mm/day

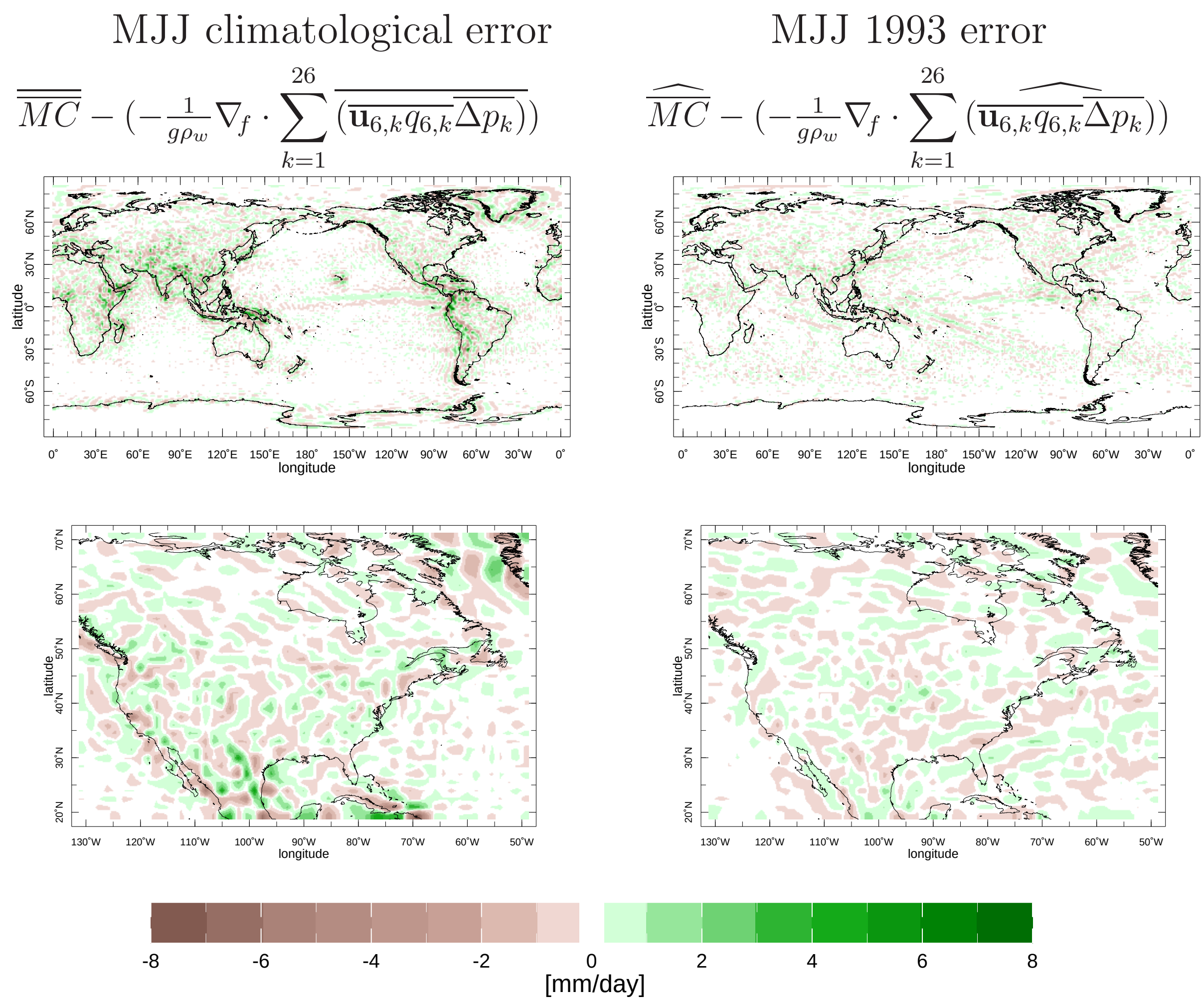

FIG. 9. The difference between ERA-I reported vertically integrated moisture convergence and that computed diagnostically with 6 hourly data on 26 levels for climatological MJJ and just for MJJ 1993 (right) . Units are mm/day

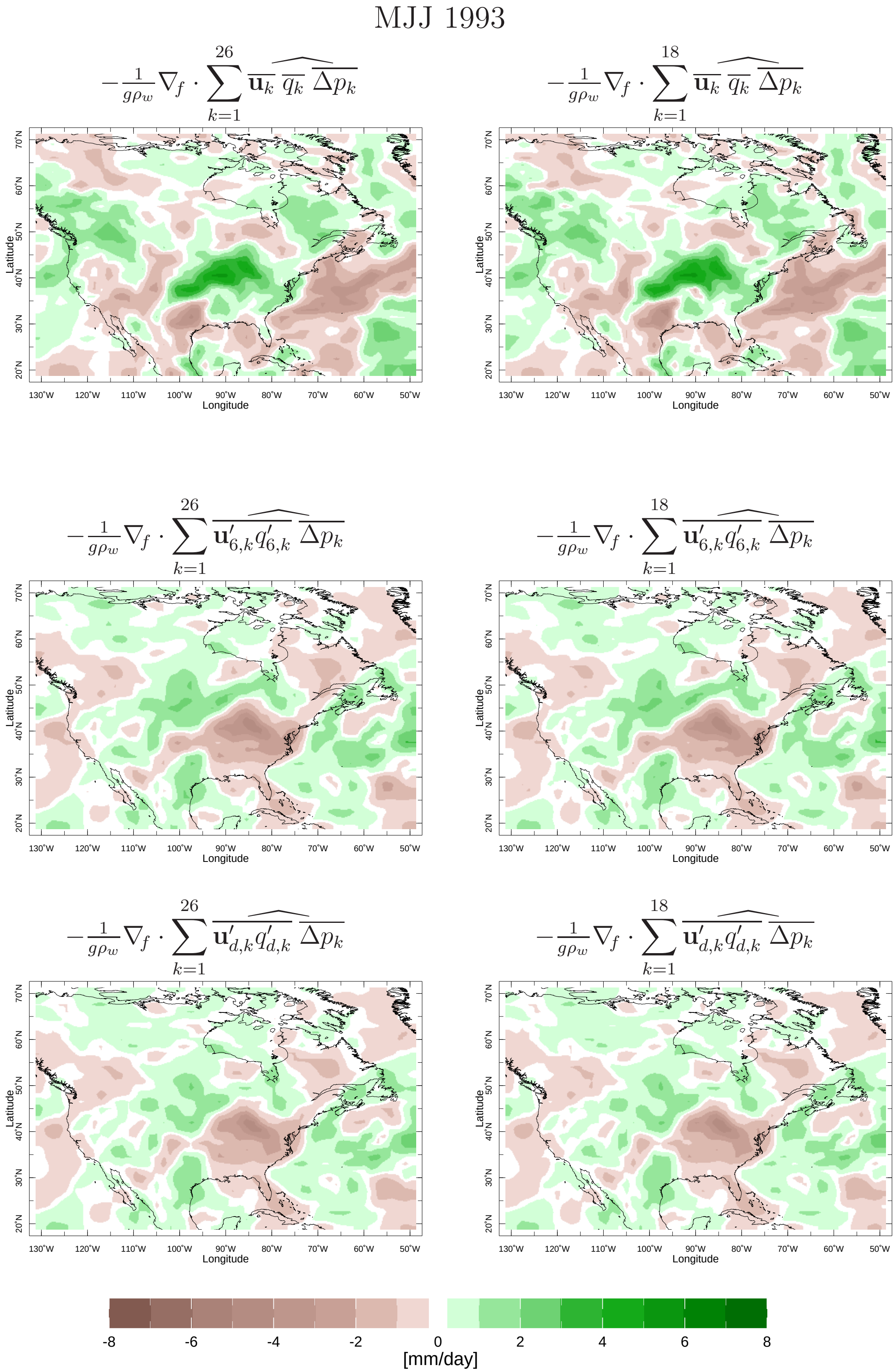

FIG. 10. Components of the MJJ 1993 moisture budget anomaly. The contribution from anomalies in the mean flow and mean humidity evaluated with 26 levels (top left) and 18 levels (top right), the contribution from transient eddy moisture flux convergence evaluated with 6 hourly data (middle) and daily data (bottom) and for 26 levels (left) and 18 levels (right). Units are mm/day

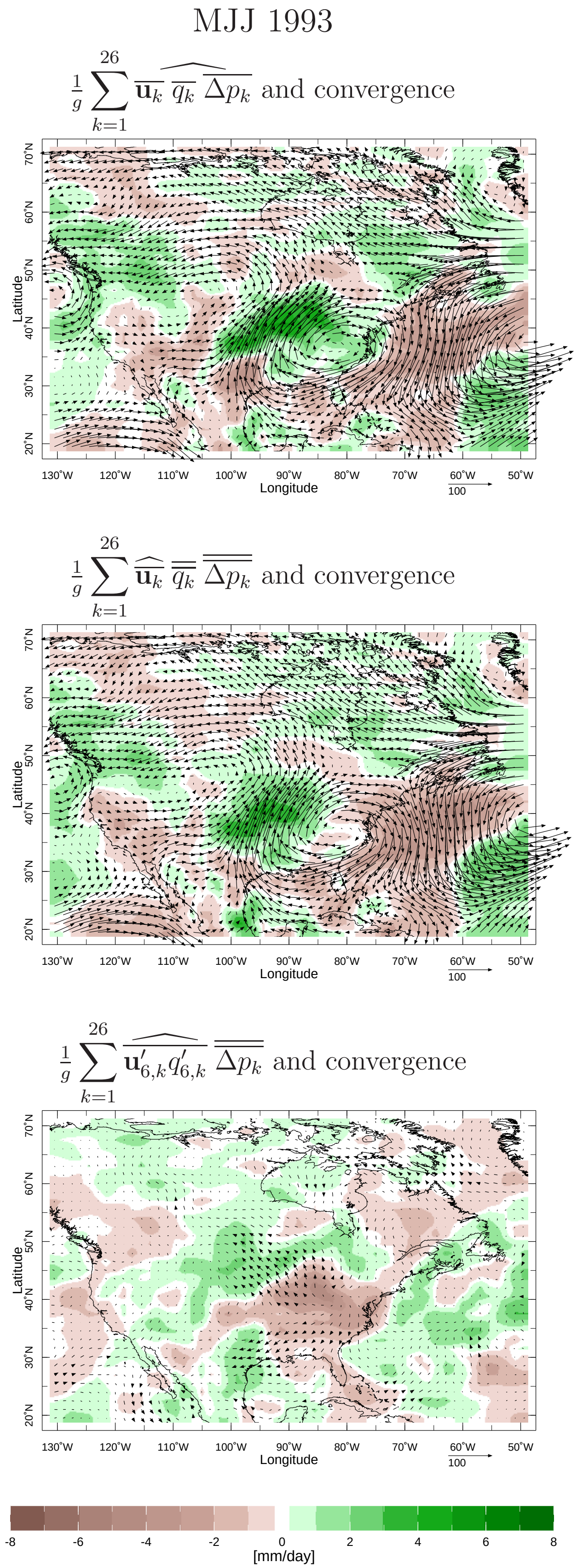

FIG. 11. The MJJ 1993 mean flow moisture flux anomaly and its convergence evaluated with 26 levels (top) and the part of this due to just mean flow anomalies combining with climatological humidity together with its convergence (middle) and the transient eddy moisture fluxes and their convergence evaluated with climatological pressure thicknesses (bottom). Units are $kg/m/s$ for the fluxes and mm/day for the convergence.

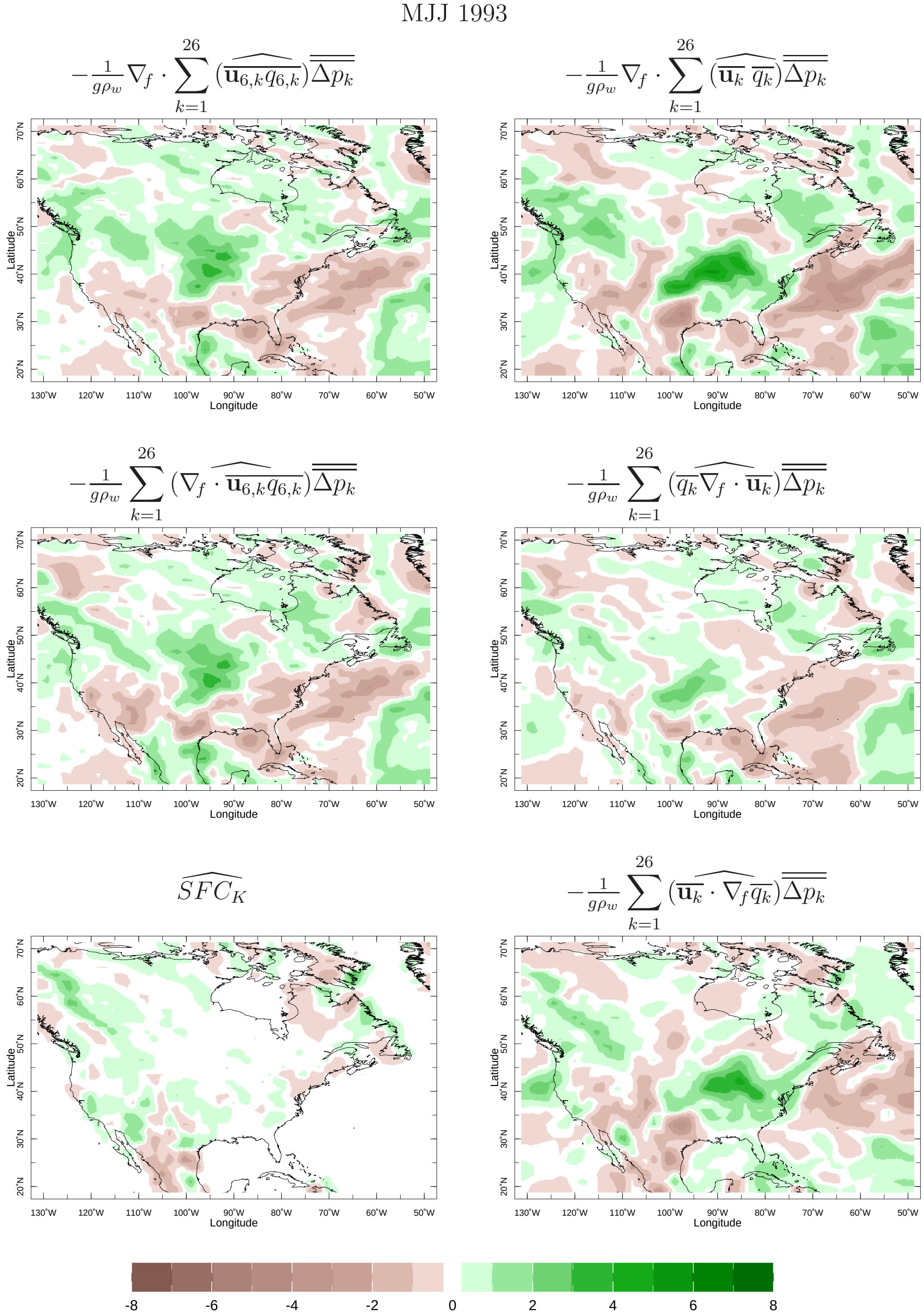

FIG. 12. The MJJ 1993 anomaly of the total convergence of the vertically integrated moisture flux (top left) and its breakdown into the vertical integral of moisture convergence (middle left) and the surface term (bottom left) all using 6 hourly data and 26 levels. The right column shows terms related to the mean flow and mean humidity anomalies. The anomaly of the convergence of vertically integrated mean flow moisture flux (top right), and the components of the vertically integrated moisture convergence due to the mean flow convergence (middle right) and mean flow advection of mean humidity (bottom right). All terms were evaluated using climatological pressure thicknesses. Units are $kg/m/s$ for the fluxes and mm/day for the convergence.

MJJ 1993

$$-\frac{1}{g\rho_w}\nabla_f\cdot\sum_{k=1}^{26}(\overline{\widehat{\mathbf{u}_{d,k}q_{d,k}}\Delta p_k})$$

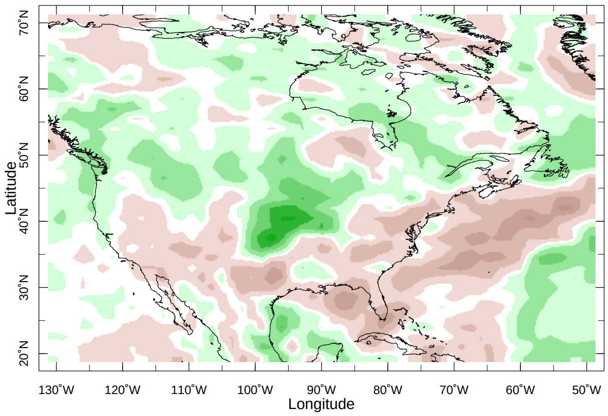

$$-\frac{1}{g\rho_w}\nabla_f\cdot\sum_{k=1}^{8}(\overline{\widehat{\mathbf{u}_{d,k}q_{d,k}}\Delta p_k})$$

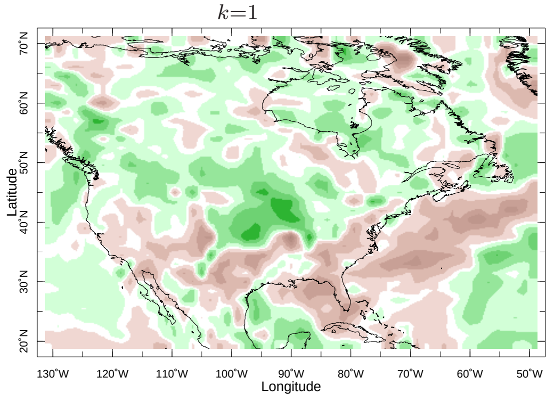

$$-\frac{1}{g\rho_w}\nabla_f\cdot\sum_{k=1}^{26}(\overline{\widehat{\mathbf{u}_{d,k}q_{d,k}}\Delta p_k}) - -\frac{1}{g\rho_w}\nabla_f\cdot\sum_{k=1}^{8}(\overline{\widehat{\mathbf{u}_{d,k}q_{d,k}}\Delta p_k})$$

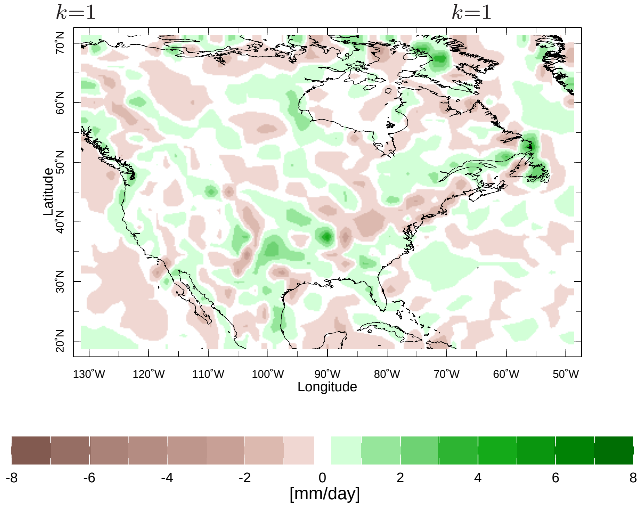

FIG. 13. The MJJ 1993 anomaly of the convergence of the total vertically integrated moisture flux computed with 26 layers (top) and 8 layers (middle) and their difference (bottom). Units are mm/day.